PB80-183866

Performance of a High-velocity Pulse-jet Filter, II

Harvard School of Public Health
Boston, MA

Prepared for

Industrial Environmental Research Lab.
Research Triangle Park, NC

Mar 80

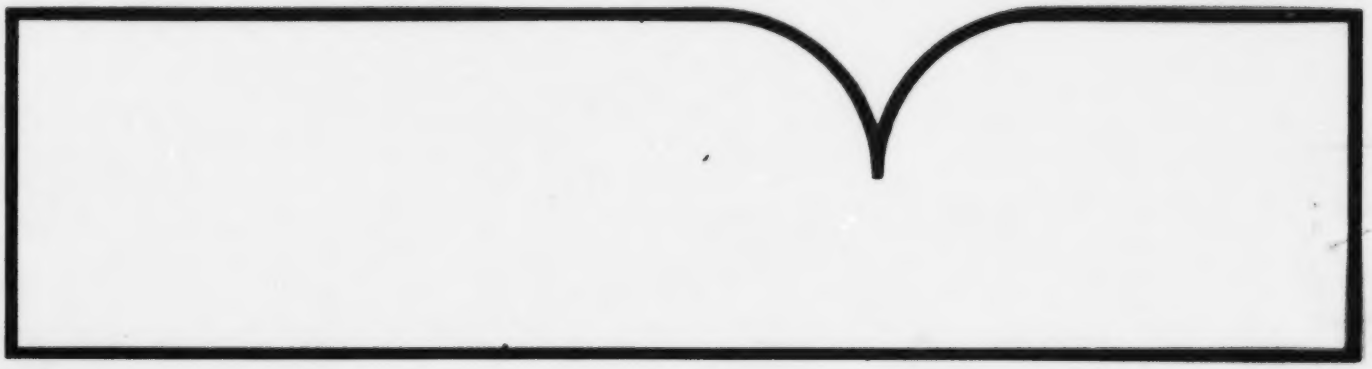

U.S. Department of Commerce
National Technical Information Service
NTIS.

PB80-143466

United States
Environmental Protection
Agency

Industrial Environmental Research
Laboratory
Research Triangle Park NC 27711

EPA-600/7-80-042
March 1980

EPA

Performance of a High-velocity Pulse-jet Filter, II

Interagency Energy/Environment R&D Program Report

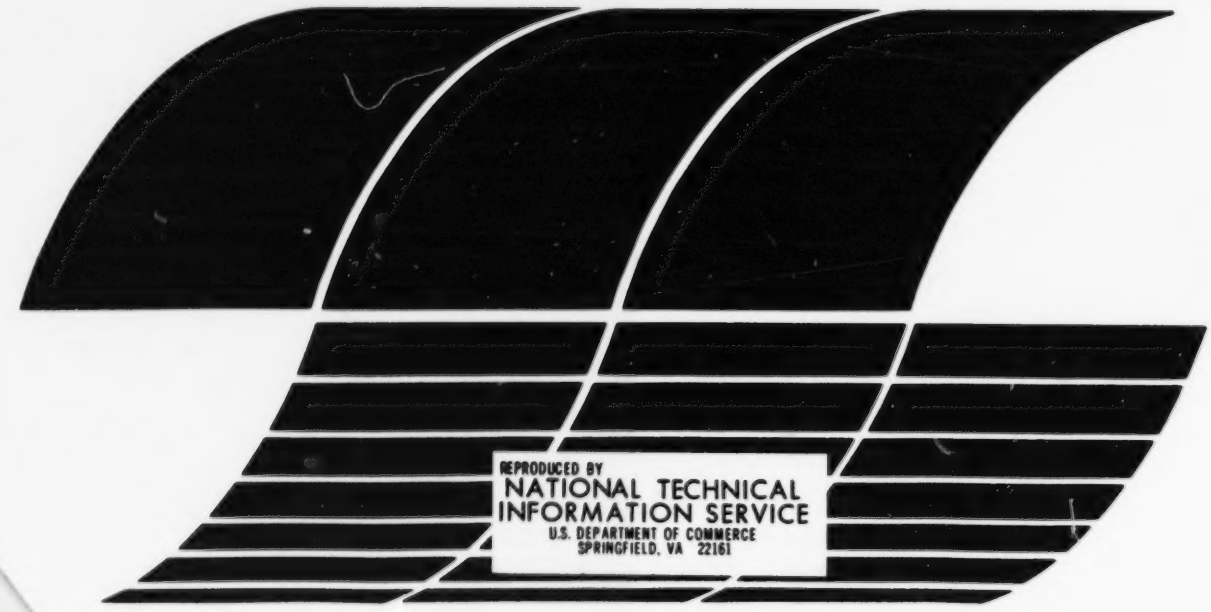

RESEARCH REPORTING SERIES

Research reports of the Office of Research and Development, U.S. Environmental Protection Agency, have been grouped into nine series. These nine broad categories were established to facilitate further development and application of environmental technology. Elimination of traditional grouping was consciously planned to foster technology transfer and a maximum interface in related fields. The nine series are:

1. Environmental Health Effects Research
2. Environmental Protection Technology
3. Ecological Research
4. Environmental Monitoring
5. Socioeconomic Environmental Studies
6. Scientific and Technical Assessment Reports (STAR)
7. Interagency Energy-Environment Research and Development
8. "Special" Reports
9. Miscellaneous Reports

This report has been assigned to the INTERAGENCY ENERGY-ENVIRONMENT RESEARCH AND DEVELOPMENT series. Reports in this series result from the effort funded under the 17-agency Federal Energy/Environment Research and Development Program. These studies relate to EPA's mission to protect the public health and welfare from adverse effects of pollutants associated with energy systems. The goal of the Program is to assure the rapid development of domestic energy supplies in an environmentally-compatible manner by providing the necessary environmental data and control technology. Investigations include analyses of the transport of energy-related pollutants and their health and ecological effects; assessments of, and development of, control technologies for energy systems; and integrated assessments of a wide range of energy-related environmental issues.

EPA REVIEW NOTICE

This report has been reviewed by the participating Federal Agencies, and approved for publication. Approval does not signify that the contents necessarily reflect the views and policies of the Government, nor does mention of trade names or commercial products constitute endorsement or recommendation for use.

This document is available to the public through the National Technical Information Service, Springfield, Virginia 22161.

TECHNICAL REPORT DATA
(Please read Instructions on the reverse before completing)

1. REPORT NO.	2.	3. RECIPIENT'S ACCESSION NO.
EPA-600/7-80-042		PB80 183866

4. TITLE AND SUBTITLE	5. REPORT DATE
Performance of a High-velocity Pulse-jet Filter, II	March 1980
	6. PERFORMING ORGANIZATION CODE
7. AUTHOR(S)	8. PERFORMING ORGANIZATION REPORT NO.
David Leith, M.J. Ellenbecker, M.W. First, J.M. Price, Anthony Martin, and D.G. Gibson	
9. PERFORMING ORGANIZATION NAME AND ADDRESS	10. PROGRAM ELEMENT NO.
Harvard School of Public Health 665 Huntington Avenue Boston, Massachusetts 02115	EHE624
	11. CONTRACT/GRANT NO.
	Grant R804700
12. SPONSORING AGENCY NAME AND ADDRESS	13. TYPE OF REPORT AND PERIOD COVERED
EPA, Office of Research and Development Industrial Environmental Research Laboratory Research Triangle Park, NC 27711	Final; 9/76-9/79
	14. SPONSORING AGENCY CODE
	EPA/600/13

15. SUPPLEMENTARY NOTES IERL-RTP project officer is James H. Turner, Mail Drop 61, 919/541-2925. EPA-600/7-78-131 includes related work.

16. ABSTRACT The report gives results of a study of the performance of a high-velocity pulse-jet filter. Such filtration has distinct advantages over low-velocity filtration in that the equipment required to clean a gas stream is reduced in size and initial cost as velocity increases. Although high filtration velocity causes a number of problems, many of them are dealt with in the report. Location of the gas inlet to the filter was found to affect penetration and pressure drop; both were higher for inlets near the bottom of the filter housing. Fabric type was also found to affect performance by affecting the amount and characteristics of the dust deposit accumulated. Fabric surface properties help explain the nature of this deposit. These ideas and others were used to develop a mathematical model for pressure drop in a pulse-jet cleaned filter. The model can be used to predict pressure drop under stable or variable operating conditions, and to predict operating conditions that cause unstable filter operation. An understanding of particle/fiber interactions is essential to understanding the collection characteristics of a felt fabric. Under certain conditions, particles bounce on impact with fibers. An adhesion probability was determined and found to depend on incident particle kinetic energy.

17. KEY WORDS AND DOCUMENT ANALYSIS

a. DESCRIPTORS	b. IDENTIFIERS/OPEN ENDED TERMS	c. COSATI Field/Group
Pollution	Pollution Control	13B
Filtration	Stationary Sources	07D
Pulsation	Fabric Filters	14B
Jets	Pulse-jet Filters	20D
Fabrics		11E
Mathematical Models		12A
Felts		
Adhesion		

18. DISTRIBUTION STATEMENT	19. SECURITY CLASS *(This Report)*	21. NO. OF PAGES
Release to Public	Unclassified	
	20. SECURITY CLASS *(This page)*	22. PRICE
	Unclassified	

EPA Form 2220-1 (9-73)

EPA-600/7-80-042

March 1980

Performance of a High-velocity Pulse-jet Filter, II

by

David Leith, M.J. Ellenbecker, M.W. First,
J.M. Price, Anthony Martin, and D.G. Gibson

Harvard School of Public Health
665 Huntington Avenue
Boston, Massachusetts 02115

Grant No. R804700
Program Element No. EHE624

EPA Project Officer: James H. Turner

Industrial Environmental Research Laboratory
Office of Environmental Engineering and Technology
Research Triangle Park, NC 27711

Prepared for

U.S. ENVIRONMENTAL PROTECTION AGENCY
Office of Research and Development
Washington DC 20460

ABSTRACT

High velocity pulse-jet filtration has distinct advantages over filtration at low velocities in that the equipment required to clean a gas stream is reduced in size and first cost as filtration velocity increases. However, high filtration velocity brings about a number of problems, many of which can be dealt with using the information presented in this report.

Experiments have shown that penetration and pressure drop increase markedly at high filtration velocities. The reasons for this involve failure to remove dust effectively from the bags and redeposition of the dust that is removed. The gas flow pattern within the filter housing should strongly affect redeposition. Using a bottom inlet to the filter housing was found to increase redeposition, and caused pressure drop and penetration to increase over values found for a top inlet filter. These increases were more pronounced at high filtration velocities.

Fabric type was also found to affect filter performance considerably. Penetration, pressure drop, dust deposited on the filter bags at equilibrium, apparent specific resistance of the dust deposit (K_2) were all studied as functions of filtration velocity and fabric type. Bags made from untreated polyester, polyester with singed surface, and ptfe laminate over polyester were used.

This and other information was used to develop a theory based on Darcy's law, which relates pressure in a pulse-jet cleaned fabric filter to characteristics of the filter and dust. The theory allows prediction of pressure drop under stable or variable operating conditions including dust concentration, filtration velocity, pulse pressure and pulse frequency, and can be used to identify operating conditions which cause pressure drop to increase without limit. Agreement between the model and experimental data is reasonably good.

Understanding of the interactions between particles and fibers is important for understanding the performance of a filter comprised of fibers made into a felt. The particle collection caracteristics of a stainless steel fibrous material collecting resuspended fly ash were investigated at high filtration velocities. Under these conditions collection effeciency by impaction should have approached 100% for all but the smallest particles present; however, contrary to classical theory, measured efficiency decreased with increasing particle size and filtration velocity. These results are explained in terms of particle bounce from the fibers on impact, and subsequent particle reentrainment. Particle-fiber behavior of the type noted here may play an important role in the penetration characteristics of high-velocity pulse-jet filters.

CONTENTS

Abstract		ii
Figures		iv
Tables		v
Acknowledgements		vi
1.	Introduction	1
2.	Conclusions	2
3.	Recommendations	4
4.	Performance of Top and Bottom Inlet Pulse-Jet Fabric Filter	5
5.	Effect of Fabric Type on Performance of Pulse-Jet Fabric Filter	12
6.	Theory for Pressure Drop in a Pulse-Jet Cleaned Fabric Filter	28
7.	High Velocity Fibrous Filtration	48

FIGURES

Number		Page
4-1	Schematic drawing of pulse-jet filter with bottom inlet (left) and top inlet (right).	7
4-2	Pressure drop vs. superficial filtration velocity, inlet location as parameter.	8
4-3	Overall mass penetration vs. superficial filtration velocity, inlet location as parameter.	9
5-1	Untreated polyester (50x).	13
5-2	Goretex^R (teflon-covered polyester) (225x).	13
5-3	Goretex^R (800x).	14
5-4	Terytex^R (singed polyester) (50x).	14
5-5	Equipment for pulse-jet filter experiments.	16
5-6	Particle size distribution for fly ash.	17
5-7	Effect of velocity and fabric on pressure drop.	20
5-8	Effect of velocity and fabric on dust penetration.	21
5-9	Effect of velocity and fabric on K_2.	22
5-10	Effect of velocity and fabric on dust deposit areal density.	23
6-1	Hypothetical relationship between fraction of dust deposit removed from fabric, ε, and area specific separation force, F_s/A.	30
6-2	Pressure drop, ΔP, vs. dust areal density added during one filtration cycle, w_0.	36
6-3	Apparatus used to determine relationship between pulse pressure, P, and induced static pressure, P_s.	38
6-4	Static pressure induced, P_s, vs. pulse pressure.	39
6-5	Equilibrium pressure drop, ΔP, vs. filtration velocity, v.	41

Number		Page
6-6	Equilibrium pressure drop, ΔP, vs. pulse pressure, P.	43
6-7	Equilibrium pressure drop, ΔP, vs. areal dust density added during one filtration cycle, w_o.	44
7-1	Theoretical single fiber impaction efficiency vs. particle diameter at 1 and 10 m/s filtration velocities.	51
7-2	High velocity filtration apparatus.	52
7-3	Fly ash penetration vs. particle size at five filtration velocities.	56
7-4	Dioctyl phthalate (DOP) penetration vs. particle size at six filtration velocities.	57
7-5	Theoretical and experimental single fiber impaction efficiencies vs. impaction parameter for DOP and fly ash.	59
7-6	Fly ash adhesion probability vs. particle kinetic energy.	61
7-7	Comparison of adhesion probability data from this study with those of other investigators.	62

TABLES

4-1	Filter characteristics.	6
5-1	Pulse-jet filter: experimental results.	19
6-1	Values of test variables used in this study.	40

ACKNOWLEDGEMENTS

Buffalo Forge Co., Buffalo, NY, donated the venturis, untreated polyester bags, and bag support cages used in this project. The polyester bags with singed surface were donated by P & S Textiles, Inc., Skaneateles Falls, NY; the polyester bags with ptfe laminate surface were donated by W. L. Gore and Associates, Inc., Elkton, MD. The contributions made by these companies are gratefully acknowledged. Dr. James H. Turner served as project officer for the grant that supported this work. His assistance with all aspects of these studies is gratefully acknowledged.

SECTION 1

INTRODUCTION

Pulse-jet cleaned filters comprise a substantial portion of the fabric filter market in the United States. However, the factors that affect filter efficiency and pressure drop are not well understood. Considerable improvement to filter performance may result from a better understanding of the factors that affect performance, and proper application of this knowledge.

This report describes research on the performance of pulse-jet cleaned fabric filters operated at high filtration velocities. This research is reported in four sections, each of which describes the results of investigations into one aspect of pulse-jet filter performance. The first section describes the effect of gas flow pattern in the filter housing on pressure drop and penetration. The second section discusses the effect of fabric type and filtration velocity on penetration, pressure drop, and fundamental factors found to determine penetration and pressure drop. The third section presents a model for pressure drop in a pulse-jet filter, which draws on understanding developed through the research described in the first two sections, and previous research.

The final section of this report is concerned with the performance of fiber filters operated at high filtration velocities. An understanding of how fibers interact with particles at high velocities is essential for understanding how nonwoven fabrics or other structures made from fibers behave under high velocity conditions.

Our approach in preparing this material has been to compose each section so that it can be read and understood independently. However, our hope is that the reader will read all the sections, since they are all aimed at the same goal - a better understanding of the factors controlling pulse-jet filter performance. Perspective gained by reading all report sections will allow best assimilation of the information we have developed while carrying out this research.

SECTION 2

CONCLUSIONS

The performance of a pulse-jet filter is adversely affected by redeposition of dust on the filter bags following a cleaning pulse. Both pressure drop and penetration increase with increased redeposition, which increases with increasing filtration velocity. High velocity filtration flow sweeps dust and agglomerates back to the bag surface more effectively than low velocity flow.

Redeposition increases when a bottom inlet configuration is used, presumably because the net upward gas flow within the filter housing reduces the effective velocity with which particles and agglomerates released by a cleaning pulse can settle to the dust hopper. Redeposition is minimized with top inlet because the gas flow is downward and dust fall toward the hopper is promoted. As a result pressure drop and penetration are minimized. For a superficial filtration velocity of 125 mm/s, filter resistance diminished by a factor of four and penetration by a factor of two when gas inlet was moved from bottom to top, all else remaining the same.

Experiments with bags made from untreated polyester, singed polyester (Terytex), and Gore-Tex laminate (over polyester) showed that pulse-jet filter performance with fly ash test dust is affected considerably by fabric choice. The dust deposit on the bag at pressure drop equilibrium was greatest for the untreated polyester, less for the singed polyester, and considerably less for the Gore-Tex.

At least two factors contribute to differences in equilibrium dust deposit. First, dust adhesion/release characteristics of the fabrics may vary, so that the amount of dust separated by a cleaning pulse varies by fabric type. Second, the abilities of the fabrics to induce particle agglomeration may vary, so that the size of the agglomerates freed by a cleaning pulse varies by fabric type. Both the amount of dust released and the size of the agglomerates released affect fabric "cleanability" and the amount of equilibrium dust deposit.

The apparent value for specific resistance of the dust deposit, K_2, was about the same for the untreated and singed polyester bags, but significantly higher for the Gore-Tex bags. The dust deposit may more closely approximate a true dust cake when collected on the smooth surface of the Gore-Tex than when collected throughout the depth of the other, more open fabrics. The apparent specific resistance of the particle-to-particle dust cake would presumably be much higher than that of a porous, particle-on-fiber deposit.

Penetration and pressure drop increased for all fabrics as filtration velocity increased. At a filtration velocity of 50 mm/s,penetration was highest for untreated bags, lowest for Gore-Tex bags; pressure drop was highest for Gore-Tex bags and lowest for untreated bags. At a velocity of 100 mm/s both penetration and pressure drop were highest for Gore-Tex bags; both penetration and pressure drop were lowest for singed bags at this velocity.

A theory for pressure drop in pulse-jet cleaned filters has been developed. With simplifying assumptions, the theory can be readily used to interpret pressure drop data or to predict the equilibrium pressure drop of a pulse-jet cleaned filter operated under any conditions. The theory also allows prediction of operating conditions under which filter operation will become unstable and cause pressure drop to increase without limit.

Particle bounce strongly affects fly ash penetration through mats of stainless steel fibers. Bounce probability increases with both increasing particle size and increasing filtration velocity. Particle adhesion probability was found to be inversely related to particle kinetic energy. These results help explain why penetration is higher than might be expected through filters made from fibers or arrays of fibers, particularly for large particles and high filtration velocities.

SECTION 3

RECOMMENDATIONS

Because pulse-jet filters operate with lower pressure drop and penetration if aerosol inlet is at the top of the filter housing, the inlet should be in this position and not at the filter bottom. This recommendation is especially important under high velocity filtration conditions. More work needs to be done to promote dust deposit separation from the filter bag, to promote separation of larger dust deposit agglomerates, and to promote active agglomerate transfer to the dust hopper so that redeposition will be minimized.

Fabric structure clearly affects pressure drop and penetration of a pulse-jet filter. The effects of fabric structure have been quantified in terms of macroscopic filtration parameters such as K_2 and residual dust loading. Considerable work remains to be done to incorporate these data in models such as the one described in this report, to allow reliable interpretation and prediction of filter penetration and pressure drop.

Penetration through pulse-jet cleaned filters increases to levels that may be unacceptable at high filtration velocities. Reasons for this may involve particle bounce or the failure of dust to adhere to the clean side of the fabric during and after cleaning. Considerable work remains to be done to relate the adhesion information presented here for fly ash particles and fiber mats to the situation found in an industrial pulse-jet filter. However, we believe that an understanding of penetration through pulse-jet filters predicted on fault processes such as particle bounce or failure of particles to adhere to fibers is more likely to explain penetration characteristics of these filters than theory based on classical particle collection mechanisms alone.

SECTION 4

PERFORMANCE OF TOP AND BOTTOM INLET PULSE-JET FABRIC FILTER

INTRODUCTION

High velocity fabric filtration has distinct advantages over filtration at low velocities in that the equipment required tc clean a gas stream is reduced in size and first cost as filtration velocity increases. However, experiments on pulse-jet cleaned filters have shown that penetration(1-4) and pressure drop(5-8) increase markedly at high filtration velocities. The reasons for this involve dust redeposition on the bags following a cleaning pulse. At high filtration velocities, most of the dust freed by a cleaning pulse is swept back to the bags rapidly, and does not fall into the hopper. As a result, a thick dust deposit develops on the bags and pressure drop increases(9). When a bag snaps back and hits its supporting cage at the end of a cleaning pulse, rapid deceleration of the fabric causes particles and agglomerates to be loosened from the dust/fabric matrix and to seep through to the cleaned gas stream when filtration resumes(3). More seepage occurs at high velocity both because the thicker redeposited dust layer provides more particles which potentially can seep through, and because high filtration velocity drives the bag against its cage faster and causes it to hit with greater impact, thereby loosening more dust from the deposit. If redeposition can be minimized in a pulse-jet filter, reductions in pressure drop and penetration should follow.

The gas flow pattern within the filter housing should strongly influence redeposition. When the filter cake is freed from the surface of a bag during a cleaning pulse, it must fall through the filter housing to reach the dust hopper. The direction and velocity of gas flowing within the housing should have a strong influence on whether this dust falls to the hopper or redeposits on a bag. When the gas in the housing helps this freed dust reach the hopper rather than hinders its transport there, redeposition should be reduced and filter performance improved.

Commercial pulse-jet filters are available with gas inlet at the bottom or top of the filter housing. A bottom inlet is

often preferred because it permits large particles to fall into the dust hopper immediately on entry and avoids their collection upon the filter bags. It is believed that this results in reduced bag wear and lower bag resistance.

EXPERIMENTS

The influence of gas motion within the filter housing on filter performance was evaluated using a three bag filter (Figure 4-1) operated at superficial filtration velocities of 50, 75, 100, and 125 mm/s with gas inlet at the top or bottom of the filter housing. Data which describe the characteristics and operation of the filter are given in Table 4-1.

TABLE 4-1. FILTER CHARACTERISTICS

Bags:	untreated polyester; 0.54 kg/m^2; 144 mm dia., 2.44 m long; 150 mm/s at 124 Pa permeability
Dust:	fly ash; count median dia. 0.3 μm, geometric standard deviation 2.7; inlet flux 9×10^{-5} kg/m^2·s; density 2200 kg/m^3
Pulses:	pressure 6.8 atm; interval once/min·bag; valve time 75 ms electrical, 240 ms mechanical

Upstream and downstream isokinetic dust samples were collected on tared glass fiber papers and used to calculate mass penetration. Replicate experiments were run in random order, except that all experiments with top inlet were concluded before experiments with bottom inlet were begun. The data presented are averages of the replicates.

RESULTS

Figure 4-2 is a plot of filter bag resistance against superficial filtration velocity for gas inlet located at the top or at the bottom of the filter housing. Although at the lowest velocity tested bag resistance was nearly the same for bottom inlet and top inlet, as velocity increased the resistance rose much more rapidly for the bottom inlet configuration. At the highest filtration velocity attained with a bottom inlet, resistance and fan energy consumption were about four times higher than for the top inlet.

Figure 4-3 is a plot of dust penetration against superficial velocity for gas inlets located at the top or bottom of the housing. Penetration was moderate at the lowest filtration velocity tested. As velocity increased, penetration increased also; however, the increase was much more rapid for the filter with bottom inlet. At the highest filtration velocities tested, penetration

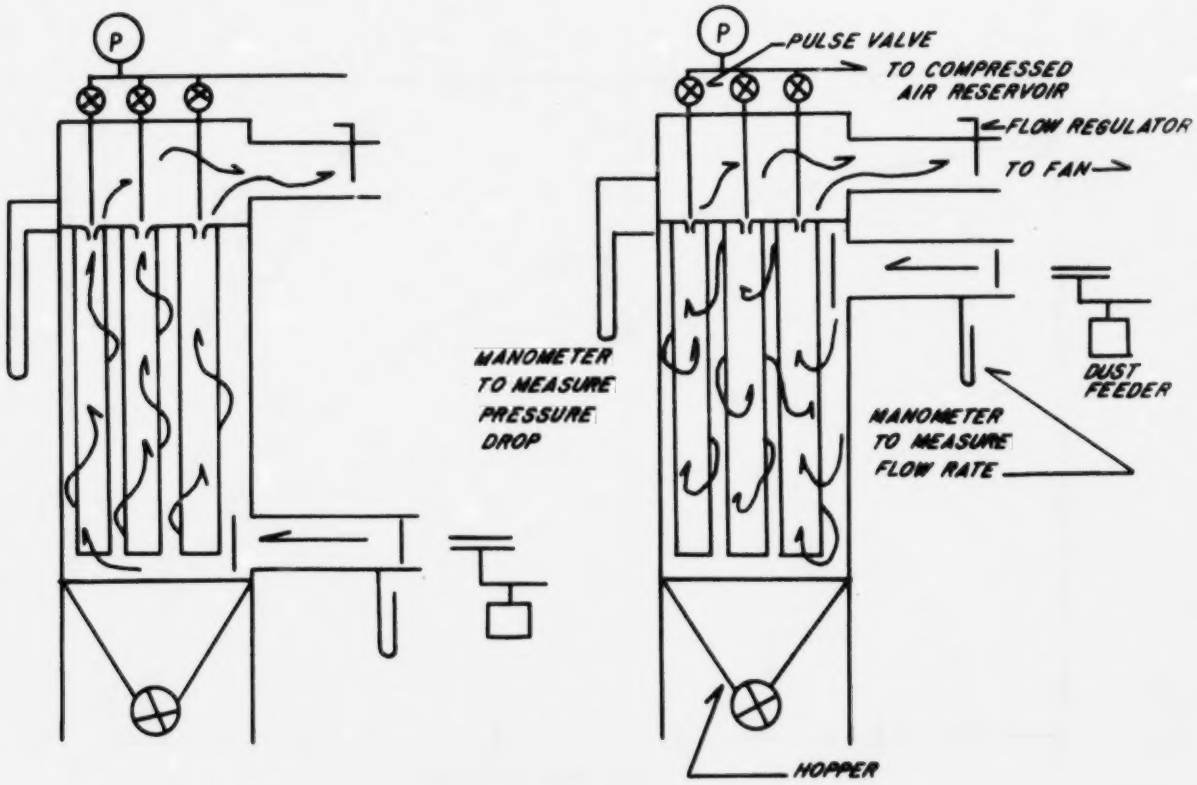

Figure 4-1. Schematic drawing of pulse-jet filter with bottom inlet (left) and top inlet (right).

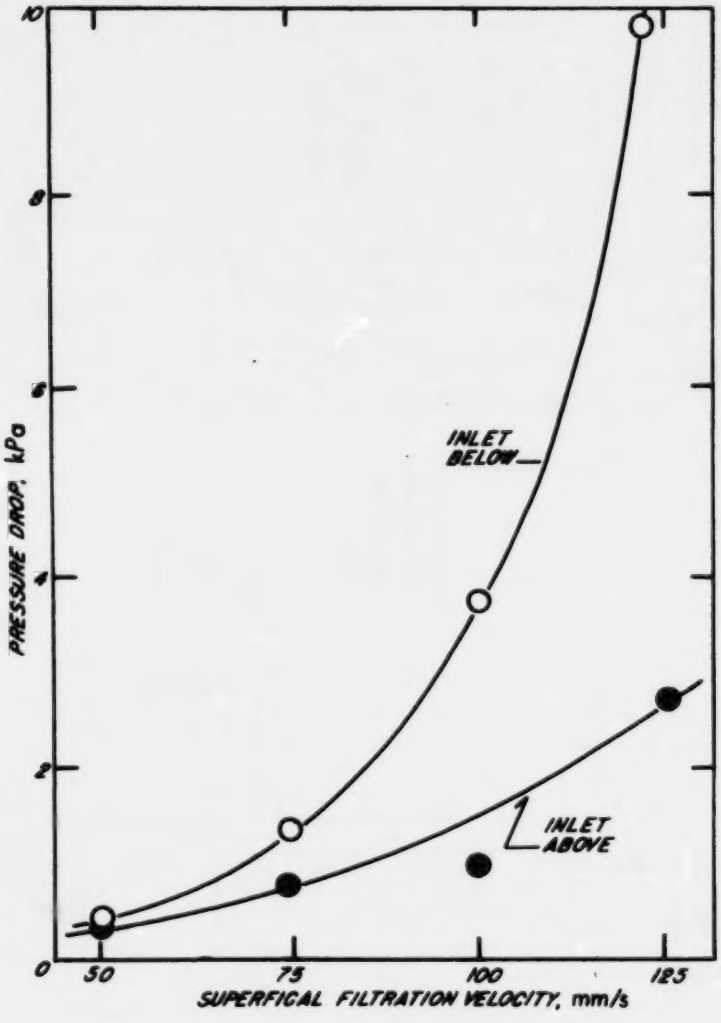

Figure 4-2. Pressure drop vs. superficial filtration velocity, inlet location as parameter.

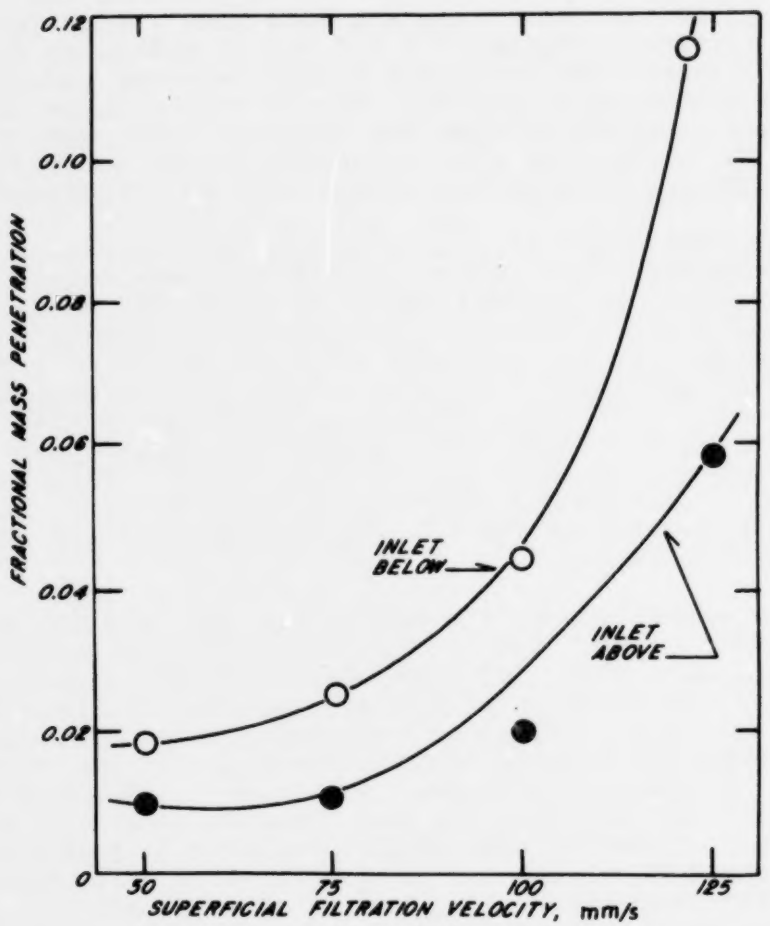

Figure 4-3. Overall mass penetration vs. superficial filtration velocity, inlet location as parameter.

became too high for many control applications with either inlet.

DISCUSSION

It will be obvious that gas inlet location has a strong influence on filter resistance and dust penetration for pulse-jet cleaned filters. Figures 4-2 and 4-3 show that as filtration velocity increases the top inlet filter performs considerably better than the bottom inlet filter. This occurs because as the volumetric gas flowrate through the baghouse increases, both the velocity of the unfiltered gas inside the filter housing, and the velocity of the gas through the filter bags also increase.

High horizontal gas velocity through the bags draws particles and agglomerates back to the bag surface immediately after a cleaning pulse and thereby causes a thick dust deposit, regardless of the gas inlet location. However, high filtration velocity also causes greater vertical gas velocity in the filter housing--downward if gas inlet is at the housing top, and upward if it is at the bottom. With top inlet, particles and agglomerates freed by a cleaning pulse are drawn toward the dust hopper by the gas flowing downward through the filter housing. With bottom inlet, gas flows upward through the filter housing. This keeps dislodged dust suspended inside the housing and permits easy redeposition on the filter bags.

With bottom entry, the net upward gas velocity within the housing will be greatest at the housing bottom where the entire gas stream must enter and flow upward to be filtered, and least at the top, by which point all process gas will have been drawn through the bags. Following a cleaning pulse dislodged dust must fall through the housing bottom, where upward gas velocity is highest. To reach the hopper, particles and agglomerates must have a terminal settling velocity greater than that of the upward moving gas. Clearly, when small particles or particles which do not agglomerate readily are to be collected in a pulse-jet filter, a gas inlet near the housing top is of substantial advantage compared to a gas inlet near the bottom. The advantage becomes greater as filtration velocity increases.

SUMMARY

The performance of a pulse-jet filter is adversely affected by redeposition of dust on the filter bags following a cleaning pulse. Redeposition increases with increasing filtration velocity because high velocity filtration flow sweeps dust and agglomerates back to the bag surface. Redeposition also increases when a bottom inlet configuration is used because the net upward gas flow within the filter housing reduces the effective velocity with which particles and aggomerates released by a cleaning pulse can settle to the dust hopper. Redeposition is minimized with top inlet because the gas flow is downward and dust fall toward the

hopper is promoted. As a result, pressure drop and penetration are minimized. For a superficial filtration velocity of 125 mm/s, filter resistance was observed to diminish by a factor of four and penetration by a factor of two when gas inlet was moved from bottom to top, all else remaining constant.

REFERENCES

1. Dennis, Richard and John Wilder. Fabric Filter Cleaning Studies. EPA-650/2-75-009, Environmental Protection Agency Office of Research and Development, Washington, 1975.

2. Mohamed, M. H., E. M. Afify and J. Vogler. Needle Punched Fabrics in Filtration. Paper presented at Technical Symposium on Nonwoven Product Technology, International Non-wovens and Disposables Association, 10 E. 40th St., New York, 1974.

3. Leith, David and Melvin W. First. Performance of a Pulse-Jet Filter at High Filtration Velocity I. Particle Collection. J. Air Poll. Control Assoc., 27:534, 1977.

4. Leith, David and Melvin W. First. Performance of a Pulse-Jet Filter at High Filtration Velocity III. Penetration by Fault Processes. J. Air Poll. Control Assoc., 27:754, 1977.

5. Holland, C. R. and E. Rothwell. Model Studies of Fabric Dust Filtration 1. Flow Characteristics of Dust Cakes Uniformly Distributed on Filter Fabrics. Filtration and Separation, 14: 30, 1977.

6. Holland, C. R. and E. Rothwell. Model Studies of Fabric Dust Filtration 2. A Study of the Phenomenon of Cake Collapse. Filtration and Separation, 14:224, 1977.

7. Leith, David and Melvin W. First. Pressure Drop in a Pulse-Jet Fabric Filter. Filtration and Separation, 14:473, 1977.

8. Bakke, Even. Optimizing Filtration Parameters. J. Air Poll. Control Assoc., 24:1150, 1974.

9. Leith, David, Melvin W. First and Henry Feldman. Performance of a Pulse-Jet Filter at High Filtration Velocity II. Filter Cake Redeposition. J. Air Poll. Control Assoc., 27:636, 1977.

SECTION 5

EFFECT OF FABRIC TYPE ON PERFORMANCE OF PULSE-JET FABRIC FILTER

INTRODUCTION

In pulse-jet cleaning of bag filters, less than 1% of the dust cake is typically removed by a single pulse(1). This is due to failure of the pulse to remove some of the dust cake and to redeposition of removed dust. Some work has been done to minimize redeposition of the dust(2,3). This report is concerned with the use of alternative bag materials designed to increase the ease of dust removal by a pulse. Three types of material were studied: untreated needled-felt polyester; Goretex®, a polyester fabric covered with ptfe and Terytex®, a needled-felt polyester whose outer surface has been singed to remove protruding fiber ends. The nominal weight of all fabrics was 0.54 kg/m^2.

Figure 5-1 is a photomicrograph of an untreated polyester bag, magnified 50 times. Although unused, this bag was slightly dirty as particles can be seen adhering to the fibers in the photograph. The average fiber diameter was 18 μm.

Figure 5-2 shows the outer surface of a Goretex bag magnified 225 times. Ptfe filaments can be seen, stretched over a matrix of polyester fibers. A large portion of the photographed area is blinded. Although this is a new bag, examination of two small samples showed this type of blockage covered a large portion, perhaps half the area, of the samples examined. Figure 5-3 is an 800X magnification of the same fabric, showing an area not affected by the blockage. The mean fiber diameter is 20 μm for the matrix and less than 1 μm for the ptfe filaments.

Figure 5-4 is a photograph of the outer surface of a Terytex bag, magnified 50 times. The melted bits of polyester, a result of the singing process, are evident. The mean fiber diameter is 19 mm.

Each type of bag was operated at several filtration velocities, and the effects of velocity and fabric on pressure drop and penetration were studied.

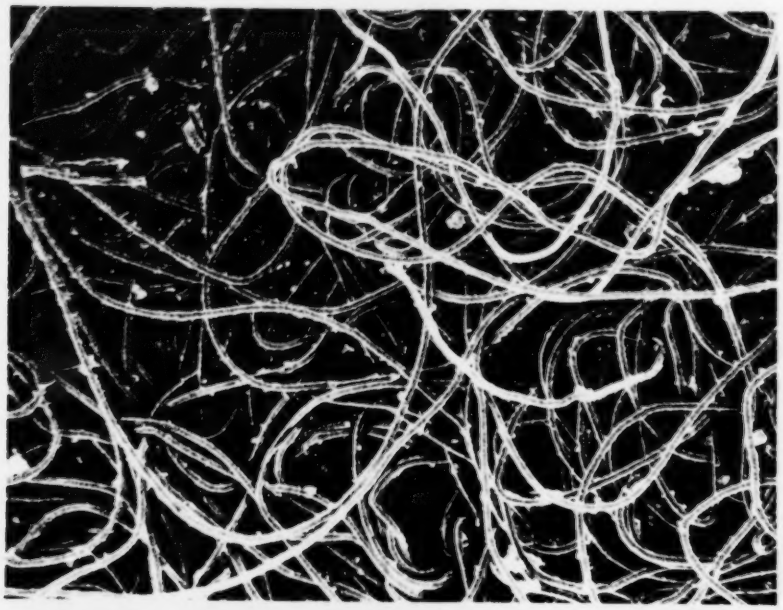

Figure 5-1. Untreated polyester (50x).

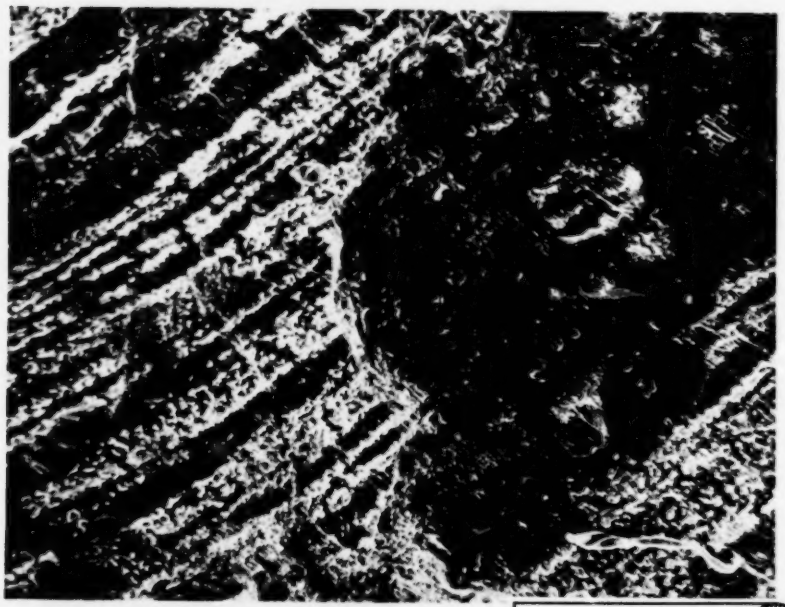

Reproduced from
best available copy.

Figure 5-2. Goretex^{R} (teflon-covered polyester)(225x).

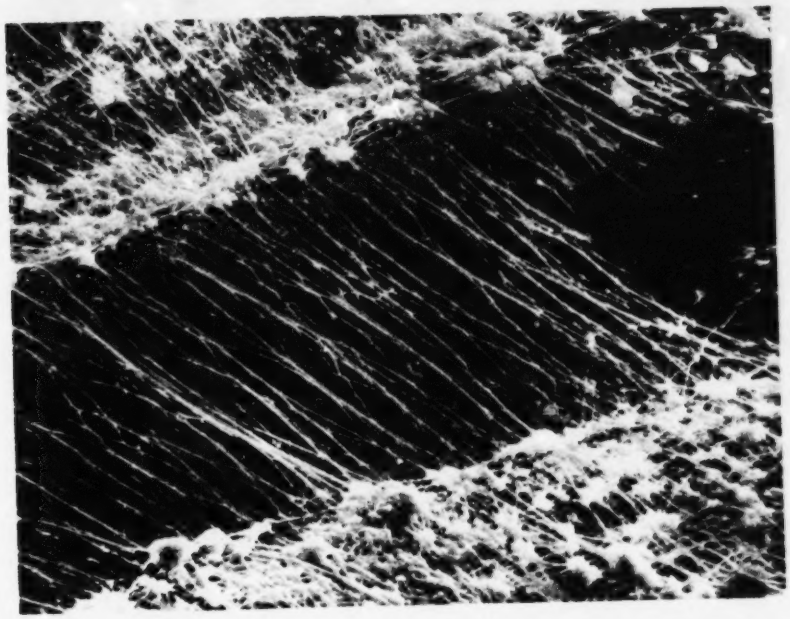

Figure 5-3. Goretex^{R} (800x).

Figure 5-4. Terytex^{R} (singed polyester) (50x).

EXPERIMENTS

The experimental apparatus is shown in Figure 5-5. Air flow through the filter is induced by a blower connected to the outlet duct. Filtration velocity is controlled by a blast gate in line with the blower. The inlet and outlet ducts are circular, 8" diameter, and the filter bags are 114 mm diameter x 2.44 m long and are supported by internal metal cages. Fly ash is measured and fed by a turntable dust feeder and is entrained in the air stream by an aspirator. The fly ash, density 2200 kg/m^3 from a coal-fired power plant, has a particle size distribution by count given in Figure 5-6. The resulting aerosol is directed into the inlet duct and passes a Stairmand disk near the entrance. The Stairmand disk(4) provides mixing of the dust with the inlet gas stream and causes a pressure drop, measured by manometer A, which increases with the air flowrate. Manometer B measures the total pressure drop across the dust deposit, bags, cages, and venturis. The bags are cleaned by pulses of 690 kPa (100 psig) compressed air. One of the 3 bags is pulsed every 20 seconds, so that each bag is cleaned once per minute. Each pulse is 250 milliseconds in mechanical duration. The dust removed from the bags falls into the hopper and is transferred via the rotary feeder into the dust bin below. Dust penetration through the bags is determined by sampling isokinetically at the upstream and downstream taps. Samples are drawn by a vacuum pump through MSA 1106-B paper for mass samples or 0.2 µm nuclepore paper for particle sizing. Relative humidity is not controlled, but is measured using a sling psychrometer. The recycle loop, shown in dashed lines, was in place during the Goretex® experiments. It was used to test the effect of recirculation on baghouse air flow patterns. These results are not discussed here.

Fifteen experiments were run with the untreated polyester bags: three replications at each of the following filtration velocities: 50, 75, 100, 125, and 150 mm/s. Equilibrium (constant pressure drop across the bags) was not achieved in any of the 150 mm/s runs. The Goretex bags were tested at 50, 100, and 150 mm/s in a total of 24 experiments. Again, none of the 150 mm/s experiments reached equilibrium. Eight experiments were completed with the Terytex bags, at the following velocities: 50, 100, 150, 175, 200 and 225 mm/s. Equilibrium was reached in all the Terytex experiments.

To determine the clean fabric resistance, K_1, a sample was cut from a new bag of each of the three materials. Each fabric sample was placed in an air stream at 5 known flowrates, and the pressure drops were measured. The slope of a plot of pressure drop versus air velocity is K_1.

Dust deposit areal densities were determined (1) from bags equilibrated under normal filter operating conditions. After equilibrium was reached, the bags were removed from their housing. Each bag was

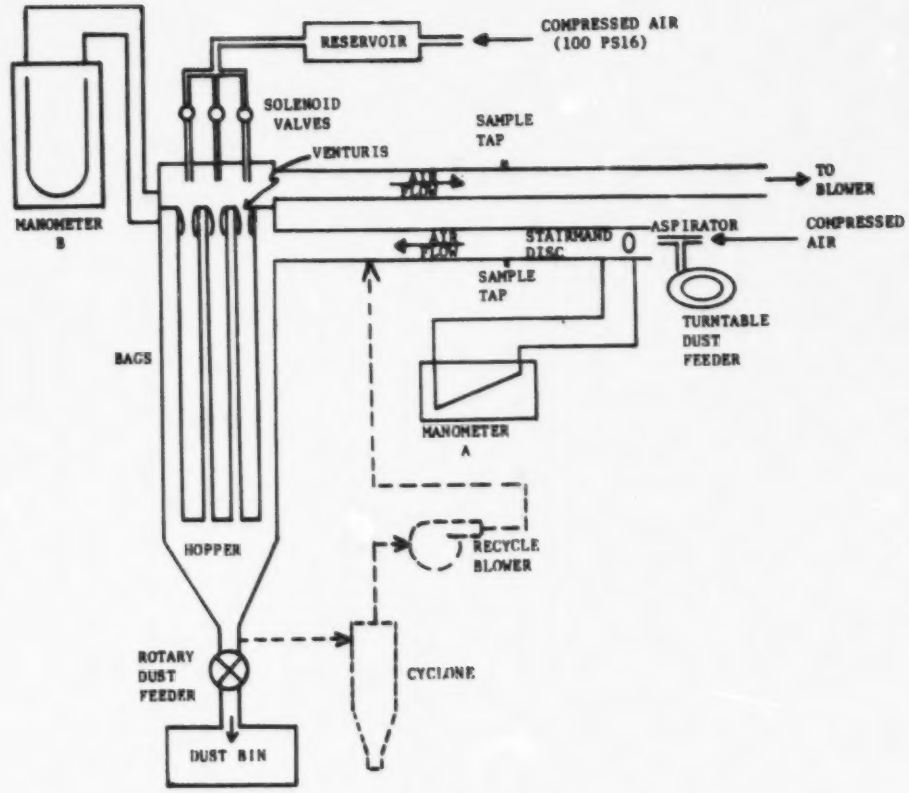

Figure 5-5. Equipment for pulse-jet filter experiments.

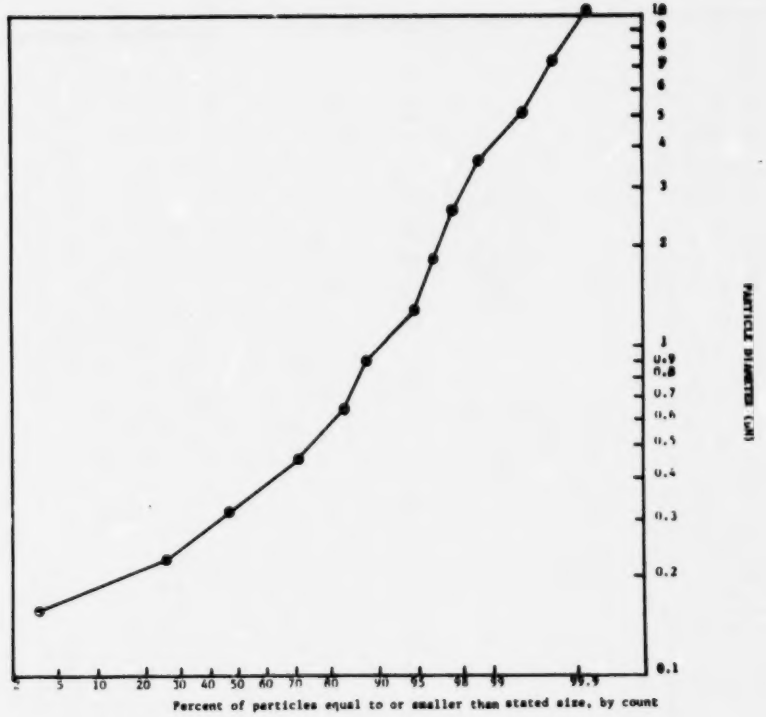

Figure 5-6. Particle size distribution for fly ash.

examined at 10 cm intervals along the bag for a total of 24 locations, by a beta gauge which measured the counts per minute of beta radiation passing through the dust deposit. The density of the dust deposit was then calculated.

RESULTS

Values of the dust deposit specific resistance, K_2, were calculated from the dust deposit areal density measurements using the method developed by Ellenbecker (1) . This method avoids the assumption of uniform dust deposit over all the bags. Each of the 3 bags was divided into 24 segments and the areal density was determined for each segment, using beta absorption and correcting the results based on the actual weight of the dust deposit. The value of K_2 was then calculated, by iteration, from the following equation:

$$\Delta p = vA\left[\sum_{i=1}^{n} \frac{A_i}{K_1 + K_2 w_i}\right]^{-1} \qquad (5\text{-}1)$$

Data and calculated values of $\bar{w}$, K_1, and K_2 are shown in Table 5-1.

Figure 5-7 is a plot of pressure drop versus velocity, and shows that pressure drop increases with velocity, and is higher for Goretex than for the other fabrics. Figure 5-8, penetration versus velocity, shows penetration increasing with velocity. Terytex generally shows the lowest penetration. Figure 5-9 shows that dust deposit specific resistance, K_2, is not strongly dependent on velocity but is dependent on fabric type. Figure 5-10 shows the dust deposit density increasing with velocity for Goretex and Terytex, but remaining roughly constant for the untreated polyester, It can also be seen that Goretex retained the least dust, Terytex retained somewhat more, and untreated polyester had the highest dust deposit areal density.

DISCUSSION

The relationships between filtration velocity and pressure drop, penetration, apparent specific resistance of the dust deposit, and areal density of the dust deposit on bags made from untreated polyester, Gore-tex, and Terytex are discussed in this section. Although the data will be discussed in terms of their dependence on filtration velocity, as for example a plot of pressure drop against velocity, the inference should not necessarily be made in all cases that velocity changes alone cause the trends plotted. For example, increased filtration velocity may increase redeposition of dust freed by a cleaning pulse, leading to a dust deposit with higher areal density. The apparent specific resistance of this deposit may then be greater as the deposit more closely approximates a true dust cake. The increases in pressure drop found with increased filtration velocity may, therefore, be more the result of changes

TABLE 5-1. PULSE-JET FILTER: EXPERIMENTAL RESULTS

		Δp(Pa)	Pt	$K_2(s^{-1})$	$\bar{w}$ (kg/m^2)	RH (%)	c_{i_3} (g/m^3)	K_1 (Pa·s/m)
POLYESTER	50 mm/s	240	.016	10,770	.3844	24	.97	850
		220	.02	8,758	.4199	22	.977	
		240	.016	12,106	.3489	28	1.08	
	75 mm/s	300	.023	8,821	.3798	29	.644	
		1470	.028	35,198	.5457	36	.644	
		420	.021	14,588	.3478	24	.72	
	100 mm/s	630	.032	14,280	.4016	26	.505	
		1630	.079	31,469	.5011	28	.433	
		580	.037	14,207	.3718	30	.494	
	125 mm/s	800	.069	17,047	.3375	27	.326	
		780	.06	17,069	.3306	20	.325	
		760	.058	12,629	.4405	28	.378	
GORETEX	50 mm/s	1957	.005			49	.84	1875
		1553	.01			28	.957	
		1425	.014	185,945	.1487	20	.9	
		2065	.009			22	.885	
		1996	.005			15	.884	
		1504	.015	184,505	.1567	16	.92	
		2095	.008	348,536	.1189	21	.846	
		2035	.009	371,918	.1075	20	.77	
	100 mm/s	3605	.046			26	.416	
		4028	.068			32	.402	
		4077	.068			20	.402	
		5120	.046			22	.372	
		3979	.065	172,698	.2219	23	.397	
		4530	.091	204,632	.2151	28	.41	
		4963	.03	344,252	.1418	18	.439	
		4943	.038	249,715	.1945	27	.407	
TERYTEX	50 mm/s	245	.015	16,455	.2757	31	.346	640
	100 mm/s	750	.011	23,797	.3089	42	.317	
	150 mm/s	2110	.024	34,752	.4153	69	.181	
		610	.024			46	.244	
	175 mm/s	1250	.046			64	.23	
		725	.039			32	.208	
	200 mm/s	680	.072			28	.193	
	225 mm/w	3525	.427	24,948	.6315	62	.125	

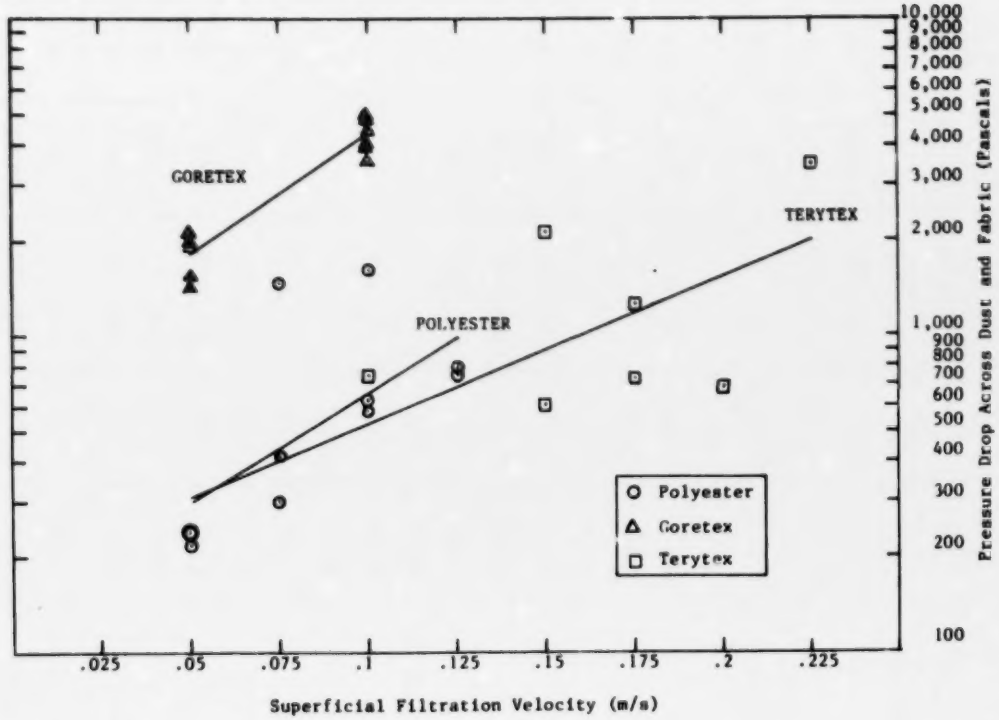

Figure 5-7. Effect of velocity and fabric on pressure drop.

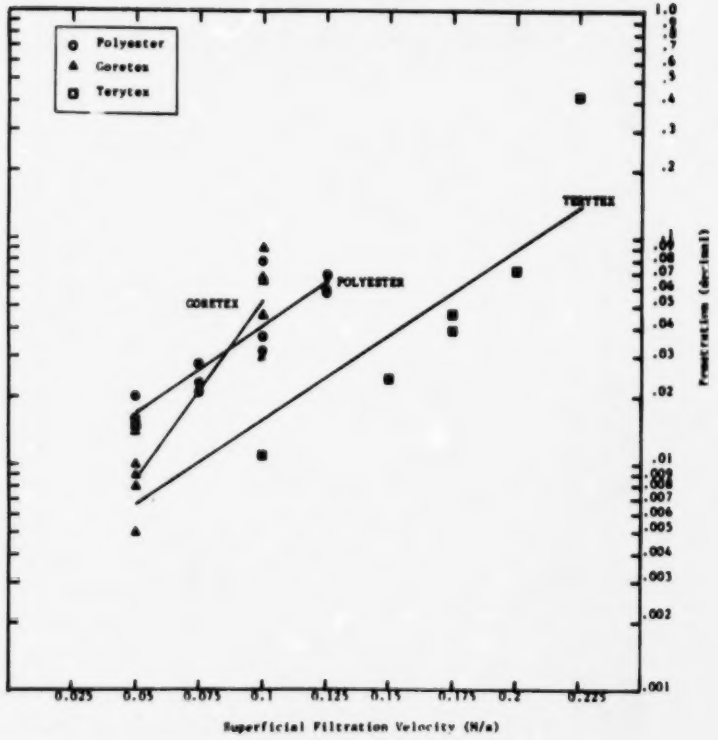

Figure 5-8. Effect of velocity and fabric on dust penetration.

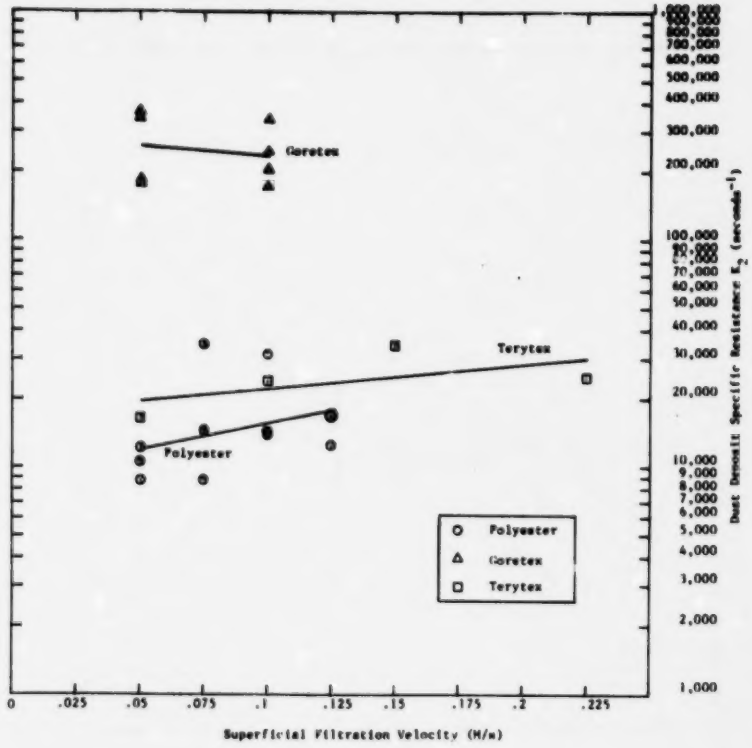

Figure 5-9. Effect of velocity and fabric on K_2.

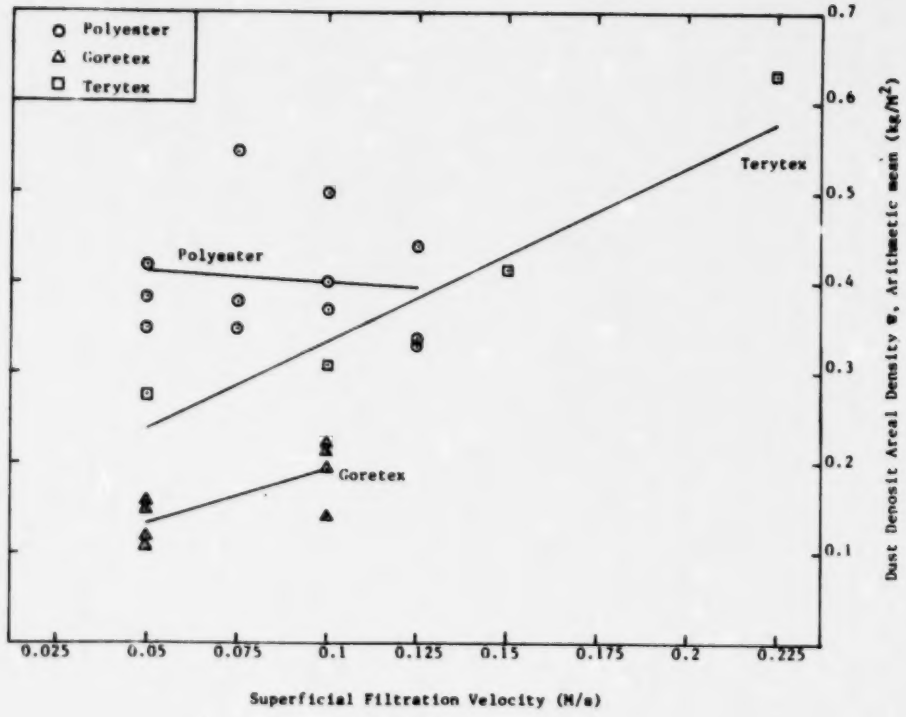

Figure 5-10. Effect of velocity and fabric on dust deposit areal density.

in the amount and characteristics of the dust deposit than the result of increased velocity through a deposit of constant properties. These relationships are discussed in more detail elsewhere (1).

Pressure Drop Versus Velocity

Figure 5-7 is a plot of pressure drop versus superficial filtration velocity, with fabric type as parameter. It shows that over the range of velocities tested, pressure drop across the Gore-tex fabric was higher than that found across either the untreated polyester or the Terytex fabrics. Although the resistance (K_1) of the new Gore-tex fabric is more than twice that for either of the other fabrics tested as shown in Table 5-1,, the comparatively high pressure drop across the clean Gore-tex fabric alone does not account for its high pressure drop in service; pressure drop across the new fabric was generally less than 10% of that across the conditioned fabric at equilibrium conditions. High pressure drop across the Gore-tex fabric bags is due to the high value of apparent specific resistance (K_2) of the fly ash dust deposits found on these fabrics. Reasons for the high K_2 values found for Gore-tex are discussed below.

Penetration Versus Velocity

Figure 5-8 is a plot of penetration versus superficial filtration velocity, with fabric type as parameter. The figure shows that penetration increases with velocity for each of the fabrics tested. Penetration through the untreated polyester and Gore-tex fabrics is somewhat higher than that through the Terytex fabric at all velocities tested.

Penetration through a pulse-jet filter may be related to impact of the cleaned bags on their supporting cages at the end of a cleaning pulse, as normal filtration resumes. Higher filtration velocity will drive the bags back to their cages faster so they hit with greater impact, thereby driving more dust through the bags and aggravating seepage. Differences in penetration for bags of different types may be explained by differences in the ability of each fabric to prevent dust from being driven through. These results suggest that Terytex bags may be more effective in this regard than either of the other fabrics tested. An additional factor which may affect penetration is the magnitude of the dust areal density on each bag. A bag with more dust on it may be likely to have more penetration both because more dust is available to seep through and because the impact with which the bag hits its cage increases with increasing dust mass; a collision with greater impact may aggravate seepage.

Apparent Specific Resistance, K_2, Versus Velocity

Figure 5-9 is a plot of the apparent dust deposit specific resistance, K_2, against superficial filtration velocity, again with

fabric type as parameter. The data indicate that apparent K_2 has very little or no dependence on superficial filtration velocity. However, the data do show considerable differences in apparent K_2 with changes in fabric type. These differences may be explained in terms of the fabric surface structure.

The surface of the untreated polyester is very open as shown in the photomicrograph, Figure 5-1. This fabric had no surface treatment. The Terytex fabric is virtually identical to the untreated polyester except that fibers protruding from the felt surface were singed as shown in the photomicrograph, Figure 5-4. The surface of the Terytex fabric is still open, but somewhat smoother than that of the untreated polyester. Gore-tex surface is much smoother than either of the other fabrics as shown in photomicrographs 5-2 and 5-3. The ptfe "mesh" which covers the surface of the polyester felt substrate for this fabric effectively precludes dust penetration into the fabric.

As a consequence, the dust deposit that develops using Gore-tex fabric most closely approximates a true dust cake in that it lies on the surface of the fabric and does not effectively penetrate the fabric interstices. This dust deposit is likely to be close-packed and compact. By comparison, the dust deposit on the surface of the Terytex and untreated polyester bags is less confined to the fabric surface, and will be based on fibers within the felt, below the fabric surface, as well as on the surface of the felt itself. The dust deposit within the felt is more likely to form inter-fiber bridges which will increase the porosity of the dust deposit which develops. A more open, porous dust deposit will have a lower specific resistance. For these reasons, the relatively smooth surface of the Gore-tex fabric leads to a dust deposit with a relatively high specific resistance, whereas the relatively rough and open surface of the untreated polyester fabric leads to a deposit with lower specific resistance. The Terytex fabric, whose surface characteristics are between those of the Gore-tex and untreated polyester, but closer to the latter, has a dust deposit with apparent specific resistance between those found on the other two fabrics, but closer to that of the untreated polyester whose surface it more closely resembles.

If a sufficiently thick dust deposit developed on the surface of even the most open, porous fabric, the specific resistance of the dust on the outside surface of this deposit would be close to that of a true dust cake. However, the surface of most felts used in pulse-jet filters, with the exception of Gore-tex, are so open and porous that it seems unlikely a dust deposit sufficiently large to approximate a cake, even at its surface, could be tolerated because of its high pressure drop. The consequence of high pressure drop would be a need for more effective cleaning to reduce the dust deposit to a less cake-like form. In this regard, pulse-jet cleaned filters differ from shaker or reverse-air cleaned filters which use woven bags, often with relatively smooth surface, and for which it is often necessary to develop a true dust cake to assure high collection efficiency.

Areal Density of Dust Deposit Versus Velocity

Figure 5-10 displays areal density of the dust deposit against superficial filtration velocity, again for each of the three fabrics tested. For the Gore-tex and Terytex fabrics, dust deposit increases with increasing velocity. This may be due to reduced effectiveness of the cleaning pulses as velocity increases. The increased operating pressure drop found under higher velocity conditions reduces the effective "reverse pressure drop" across the bags generated by the cleaning pulses, necessary to expand the bags outward and cause cleaning. An alternative explanation is that under high velocity conditions more freed dust redeposits at the end of a cleaning pulse rather than falls to the dust hopper. This causes each pulse to be less effective at cleaning dust from the bag as velocity increases, although the amount of dust momentarily freed from the bag may remain the same. The relative insensitivity of areal density to filtration velocity for the untreated polyester felt is perplexing. Additional data, taken at higher velocity than the data shown here, do demonstrate an increase in areal dust denisty with velocity for this velocity (1).

SUMMARY

The performance of a pulse-jet filter using bags made from various materials, as determined by variations in dust penetration and filter pressure drop, clearly changes with increasing filtration velocity. Many of these changes are related to differences in the properties of the dust deposit such as its magnitude or apparent specific resistance, and to differences in the characteristics of the fabric itself such as its surface properties or clean-flow resistance. Although qualitative explanations of performance data presented here can be made in terms of dust deposit and fabric properties, more satisfactory, quantitative explanations are not always possible at this time due to our incomplete understanding of the processes involved. The data presented and discussed here are for collection of fly ash. The conclusions reached might or might not be similar if another dust were to be used, as the relationships between dust properties and filter performance are, at present, incompletely understood.

NOMENCLATURE

A	area of filter bag, square meters
A_i	area of segment of filter bag, square meters
C_i	inlet concentration, grams/square meter
K_1	clean fabric resistance, pascal seconds/square meter
K_2	dust deposit specific resistance, seconds^{-1}
n	number of filter bag segments
ΔP	pressure drop across bag and dust deposit, pascals
P_t	penetration (decimal)
RH	relative humidity, per cent
v	superficial filtration velocity, meters/second
w	dust deposit areal density, kilograms/square meter
$\bar{w}$	arithmetic mean areal density, kilograms/square meter

REFERENCES

1. Ellenbecker, M.J. Pressure Drop in a Pulse-Jet Fabric Filter. Sc.D. Thesis, Harvard School of Public Health, Boston, Ma., 1979.

2. Leith, David, Melvin W. First and Dwight D. Gibson. Performance of a Pulse-Jet Filter at High Filtration Velocities. In: Symposium on the Transfer and Utilization of Particulate Control Technology, Volume 2, EPA-600/7-79-944b, NTIS, Springfield, Va., 1979.

3. Leith, David, Melvin W. First and Dwight D. Gibson. Effect of Modified Cleaning Pulses on Pulse-Jet Filter Performance. Filtration and Separation, September-October 1978, pp. 400-406.

4. Stairmand, C.J. Sampling Gas-Borne Particles. Engineering, 41:141, 1941.

SECTION 6

THEORY FOR PRESSURE DROP IN A PULSE-JET CLEANED FABRIC FILTER

INTRODUCTION

Pressure drop through gas cleaning equipment is an important component of system operating cost. For this reason, knowledge of the factors that affect pressure drop, and methods for pressure drop prediction are important. The characteristics of gas flow through a porous medium, fundamental to modeling pressure drop in a fabric filter, have been well studied(1-5). Much of this work concerns flow through a particle deposit with known properties such as pore size and porosity. With this information, dust deposit specific resistance, K_2, the pressure drop per unit velocity and per unit deposit thickness, can be predicted. Rudnick(5,6) has shown that K_2 can be estimated using an adaptation of the Happel unit cell model(7). This approach gives much better agreement with data for the usual case where dust deposit porosity is greater than about 0.8 than does the Kozeny and Carman model frequently used(8).

Before these theories can be applied to a practical fabric filter, it is necessary to consider the pressure drop contribution of the dust-conditioned fabric, and to account for the effect of incomplete fabric cleaning. Some models propose that virtually all dust is removed from a woven fabric cleaned by shaking or reverse air(9,10). However, experimental work by Dennis et al.(11, 12) demonstrated that virtually all dust is removed only from some portions of woven fabrics cleaned by these methods, and that other portions are apparently not cleaned at all. As cleaning intensity increases, the ratio of cleaned to uncleaned areas increases. Dennis et al. described a model which utilized these ideas for predicting pressure drop in a filter using woven cloth cleaned by shaking or reverse air(13).

The fabric characteristics and cleaning method for a pulse-jet filter with felt bags cleaned on-line are considerably different from those of a shaker cleaned filter, so that carryover of the model proposed by Dennis et al. is inappropriate. For a filter with woven bags cleaned off-line by shaking, more than half the dust is usually removed(12). For a pulse-jet filter with felt

bags cleaned on-line, one percent or less of the dust on a bag may be removed per pulse, and this percentage may decrease as filtration velocity increases(14-16). For a shaker cleaned filter, dust separates from the fabric in patches(11,13). For a pulse-jet filter, the distribution of dust on the bags after cleaning is almost uniform(14). Off-line shaker cleaning allows time for the separated dust to fall to the hopper before filtration resumes, whereas when a pulse-jet filter is cleaned on-line in a fraction of a second, separated dust has little time to fall to the hopper. Much of the separated dust may redeposit on neighboring bags or on the pulsed bag(16). Bag spacing, dust type, pulse characteristics, bag tension, housing design and gas flow pattern within the housing may all affect dust redeposition in a pulse-jet filter(12,17).

Empirical models(18,19) have been used to describe pressure drop(Δp). One such model(19) developed for fly ash collected on polyester bags for a range of filtration velocities, v, pulse pressures, P, and areal dust densities added during a filtration cycle, w_0, is:

$$\Delta p \propto \frac{v^{2.34} w_0^{0.45}}{P^{1.38}} \qquad (6\text{-}1)$$

in which

$$w_0 = c_1 vt \qquad (6\text{-}2)$$

Here, c_1 is inlet dust concentration and t is time between pulses to each bag.

This paper presents a theoretical treatment of pressure drop in a pulse-jet filter. In the development, some assumptions must be made which should be reexamined as data become available.

DUST SEPARATION FROM FABRIC

First, consider the forces which bind dust to the fabric. If a certain separation force per unit area, F_s/A, were applied to this dust deposit in the appropriate direction, a certain fraction, ε, would be separated. A hypothetical distribution of these unit area forces is plotted in Figure 6-1 as ε vs. F_s/A. The exact shape of this curve is unknown, but it should pass through the origin as no dust will be separated if no force is applied. The value of ε should approach unity as an asymptote, because the incremental effect of additional force is likely to diminish after most of the dust has been removed. Similar curves were developed by Dennis and Wilder (12) for woven fabrics cleaned by shaking. They show filter capacity (dust mass removed by cleaning) vs. bag acceleration during the cleaning process.

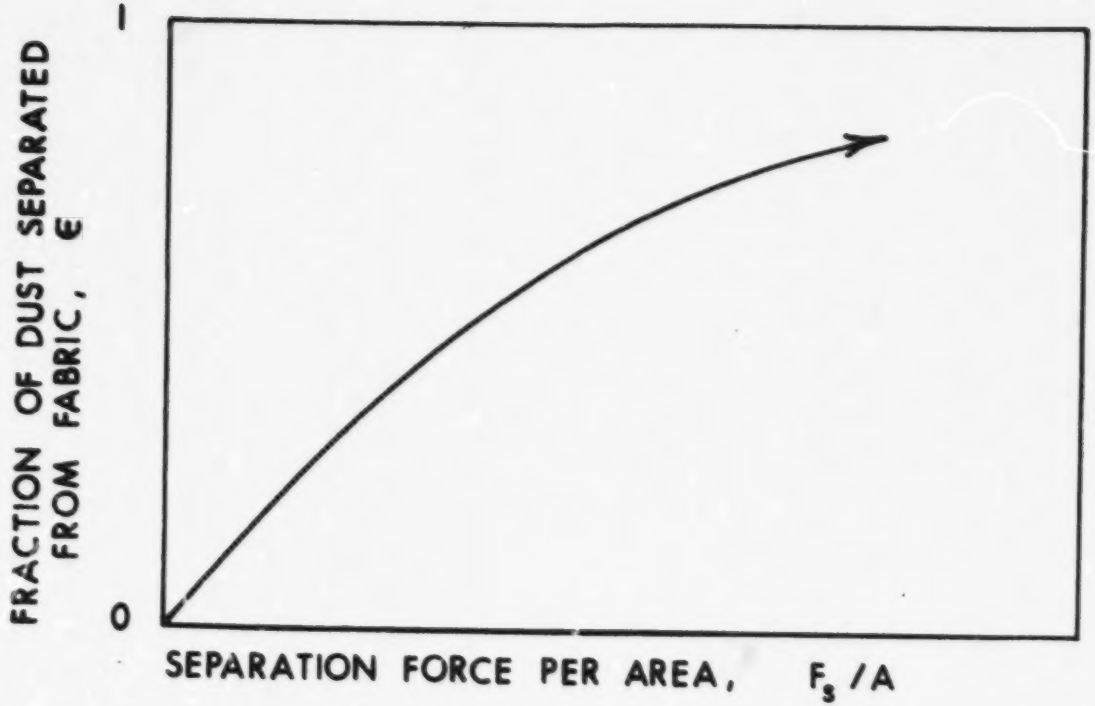

Figure 6-1. Hypothetical relationship between fraction of dust deposit removed from fabric, ε, and area specific spearation force, F_s/A.

For pulse-jet cleaned filters, experimental measurements demonstrate that ε is less than a few percent(14-16). For lack of better information, it may be assumed that the relationship between ε and F_s/A is a simple proportionality:

$$\varepsilon = kF_s/A \tag{6-3}$$

Next, consider the interaction of separating forces with the dust deposit and fabric. The net force per unit fabric area during cleaning which drives the fabric and dust away from the cage that supports them during filtration will be called the reverse pressure drop, Δp_r; it is the difference between the static pressure developed by the pulse within the bag, P_s, and the operating pressure drop across the bag at the time the pulse begins, Δp:

$$\Delta p_r = P_s - \Delta p \tag{6-4}$$

If the jet pulse develops a maximum pressure less than the pressure drop across the bag ($P_s < \Delta p$) the bag will not expand, no reverse air will flow through it, and no cleaning will take place.

As cleaning begins, fabric and dust receive an impulse which drives both away from the wire cage and both attain a certain momentum. Division of the impulse/momentum equation by bag area gives:

$$\Delta p_r t_1 = v^*(w_b + w) \tag{6-5}$$

Here, t_1 is the time over which Δp_r acts, v^* is the outward velocity attained, w_b and w are the areal density of the clean bag and the dust deposit, respectively.

The area specific force, F_s/A, which acts to separate dust from the fabric can be found from the impulse necessary to stop the outward momentum of the dust deposit:

$$\frac{F_s t_2}{A} = v^* w \tag{6-6}$$

Substitution of Equations (6-4) to (6-6) into Equation (6-3) yields an expression for the fraction of dust which is separated from the fabric by a cleaning pulse:

$$\varepsilon = \frac{(P_s - \Delta p) t_1 k}{t_2} - \frac{v^* w_b k}{t_2} \tag{6-7}$$

or

$$\varepsilon = K_3(P_s - \Delta p) - K_4 \tag{6-8}$$

Constant K_3 expresses the effectiveness with which reverse pressure

drop interacts with the bag to remove dust; K_4 expresses the effect of reverse fabric motion. Strangert(20) reports that increased reverse pressure drop increases cleaning effectiveness.

Dust separated from the fabric must fall to the hopper to be removed from the system. However, some separated dust may redeposit on the fabric before reaching the hopper, and cause actual fractional separation to be less than that predicted by Equation 6-3. Redeposition may cause the effective value of constant K_3 in a full-size filter to depend on factors that affect redeposition, such as filtration velocity, housing design, or other variables. The present model does not account for the effect of redeposition; further work on this subject is planned.

AREAL DENSITY OF DUST DEPOSIT

Models for the pressure drop across a woven fabric generally assume that total drop equals the sum of losses across the conditioned fabric, K_1v, and across the dust deposit, K_2vw.

$$\Delta p = K_1 v + K_2 v w \tag{6-9}$$

K_1 is the resistance of the fabric after it has been operated for some time and is well conditioned with dust, K_2 is the specific resistance of the dust deposit, and w is the areal density of the dust deposit on the bags.

A mass balance for the dust mass per unit area on a bag can be written for one filtration cycle, dN, which includes by definition exactly one cleaning pulse:

Additional areal density due to dust added to the bag per cycle	-	Decrease in areal density due to dust removed from the bag per cycle	=	Accumulation of areal density on the bag per cycle

$$w_0 - w\varepsilon = \frac{dw}{dN} \tag{6-10}$$

Substitution of Equations (6-8) and (6-9) into Equation (6-10) gives:

$$\frac{dw}{dN} = (K_2K_3v)w^2 + (K_1K_3v - K_3P_s + K_4)w + w_0 \tag{6-11}$$

This can be solved after the following substitutions are made:

$$a = -w_0 \tag{6-12}$$

$$b = K_3P_s - K_1K_3v - K_4 \tag{6-13}$$

$$c = -K_2K_3v \tag{6-14}$$

$$q = (K_3P_s - K_1K_3v - K_4)^2 - 4w_0K_2K_3v \qquad (6\text{-}15)$$

The solution to Equation (6-11) is:

$$w = \frac{b - \sqrt{q} - (b + \sqrt{q})F(N)}{2c(F(N)-1)} \qquad (6\text{-}16)$$

in which

$$F(N) = \left(\frac{2cw_i + b - \sqrt{q}}{2cw_i + b - \sqrt{q}}\right) \exp(-N\sqrt{q}) \qquad (6\text{-}17)$$

Here w_i is the initial areal density, the areal density of the dust deposit at N = 0, the beginning of the first filtration cycle when operating conditions are changed. Equation (6-16) gives the areal density of the dust deposit on the bag at any time; that is, at any number of filtration cycles, N, since operating conditions are changed and cycle counting begins.

EQUILIBRIUM

If operating conditions are constant, Equation (6-16) can be used to determine the value of areal dust density that the filter will achieve at equilibrium ($N \to \infty$). In this case, Equation (6-17) shows that $F(N) \to 0$ and Equation (6-16) becomes:

$$w = \frac{-b + \sqrt{q}}{2c} \qquad (6\text{-}18)$$

or

$$w = \frac{P_s - K_4/K_3 - K_1v}{2K_2v} - \frac{\sqrt{(P_s - K_4/K_3 - K_1v)^2 - 4w_0vK_2/K_3}}{2K_2v} \qquad (6\text{-}19)$$

Substitution of Equation (6-19) into Equation (6-2) gives equilibrium pressure drop:

$$\Delta p = \frac{P_s - K_4/K_3 + K_1v}{2} - \frac{\sqrt{(P_s - K_4/K_3 - K_1v)^2 - 4w_0vK_2/K_3}}{2} \qquad (6\text{-}20)$$

SUBSTITUTION

Experiments have established that under certain operating conditions pressure drop across a pulse-jet filter does not stabilize but increases without limit. Mathematically, this is equivalent to a situation in which F(N) = 1, as can be seen by inspection of Equation (6-16). Solution of Equation (6-17) for this condition gives the following criterion, which must be satisfied for stable filter operation:

$$2cw_i + b + \sqrt{q} > 0 \qquad (6\text{-}21)$$

or

$$P_s + \sqrt{(P_s - K_4/K_3 - K_1 v)^2 - 4w_0 v K_2/K_3} - 2K_2 v w_i - K_1 v - K_4/K_3 > 0 \qquad (6\text{-}22)$$

The square root term within Equation (6-22) contains terms related to the characteristics of the filter, K_1 through K_4, and to the conditions under which it is operated, P_s, v, and w_0, and must be real if stable filter operation is to be possible:

$$(P_s - K_4/K_3 - K_1 v)^2 - 4w_0 v K_2/K_3 > 0 \qquad (6\text{-}23)$$

If Equation (6-23) is not satisfied, the characteristics of the filter or its operating conditions must be changed.

The balance of Equation (6-22) contains variable w_i, the areal density of the dust deposit at time zero. If this term is sufficiently large, that is, if too much dust is on the bags, the stability criterion given by Equation (6-22) will not be met and pressure drop will increase without limit. However, for the same filter and operating conditions, stability may be achieved if the initial areal density is low enough. This has practical implications for fabric filter operation. Before operating conditions such as filtration velocity, v, dust type, K_2, or pulse pressure, P_s, are changed, the bags should be pulsed repeatedly to remove as much dust as possible and decrease w_i. This will give the best opportunity for the system to achieve stable operation under the new operating conditions.

Equation (6-22) can be rewritten:

$$\Delta p_i < \Delta p_L \qquad (6\text{-}24)$$

where

$$\Delta p_i = K_1 v + K_2 v w_i \qquad (6\text{-}25)$$

and

$$\Delta p_L = \frac{P_s - K_4/K_3 + K_1 v}{2} + \frac{\sqrt{(P_s - K_4/K_3 - K_1 v)^2 - 4w_0 v K_2/K_3}}{2} \qquad (6\text{-}26)$$

The actual operating pressure drop, Δp_i, immediately after operating conditions change must not exceed a certain limiting pressure drop, Δp_L, defined by Equation (6-26). If Δp_i is higher than Δp_L, then the system is unstable and pressure drop will increase without limit. If, however, Δp_i is lower than this quantity, then the system will be stable and approach pressure drop equilibrium.

For example, a filter might have a stable, equilibrium pressure drop of 1000 Pa under a particular set of operating conditions. Pulse pressure might then be reduced, causing a reduction in P_s, and in Δp_L as predicted by Equation (6-26). In this case, the initial pressure drop under the new conditions Δp_1 (here equal to 1000 Pa) may now be greater than Δp_L, and violate the stability condition set by Equation (6-24). If this occurs, pressure drop would rise from its initial value of 1000 Pa and increase without limit. However, if the reduction in P_s had been less, the value for Δp_L calculated in Equation (6-24) would be greater and the stability condition given in Equation (6-22) might still be satisfied. In that case, pressure drop would still rise from its initial value of 1000 Pa, but would eventually come to equilibrium.

Figure 6-2 is a plot of pressure drop, Δp, as given by Equation (6-20) against w_0, the dust areal density added during a filtration cycle for typical operating conditions. The figure shows that as more dust is fed to the bags between pulses, either by increasing inlet dust concentration or by increasing the time between cleaning pulses, equilibrium pressure drop increases as well. At the maximum value of w_0 for which stable filter operation is possible, the value of $d(\Delta p)/dw_0$ becomes infinite; that is, a slight increase in w_0 causes equilibrium pressure drop to increase at an infinite rate. This point is at the edge of the unstable region defined by Equation (6-23).

Also shown in Figure 6-2 is a plot of Δp_L, the maximum initial pressure drop for which the filter will ultimately achieve stable operation, given by Equation (6-26). Comparison of Equation (6-26) and Equation (6-20) for equilibrium pressure drop shows they are identical except for the sign on the square root term.

The arrows shown in Figure 6-2 represent the direction in which pressure drop will proceed over time and pulses, starting at any point on the figure. The arrows were determined by evaluating the derivative of areal density with respect to number of pulses at various points. For all initial conditions leading to pressure drops within the parabola shown in Figure 6-2, pressure drop will decrease to reach equilibrium. For all initial conditions leading to pressure drops outside the parabola, pressure drop will increase either until it intersects the parabola and reaches equilibrium, or else without limit.

COMPARISON WITH DATA

The static pressure increase within a bag during cleaning, P_s, is related to the rate at which air is forced backwards through the bag during cleaning. For a jet-pump, this flowrate depends in part upon jet pressure. The relationship between pulse pressure and static pressure developed, P_s, was determined for a

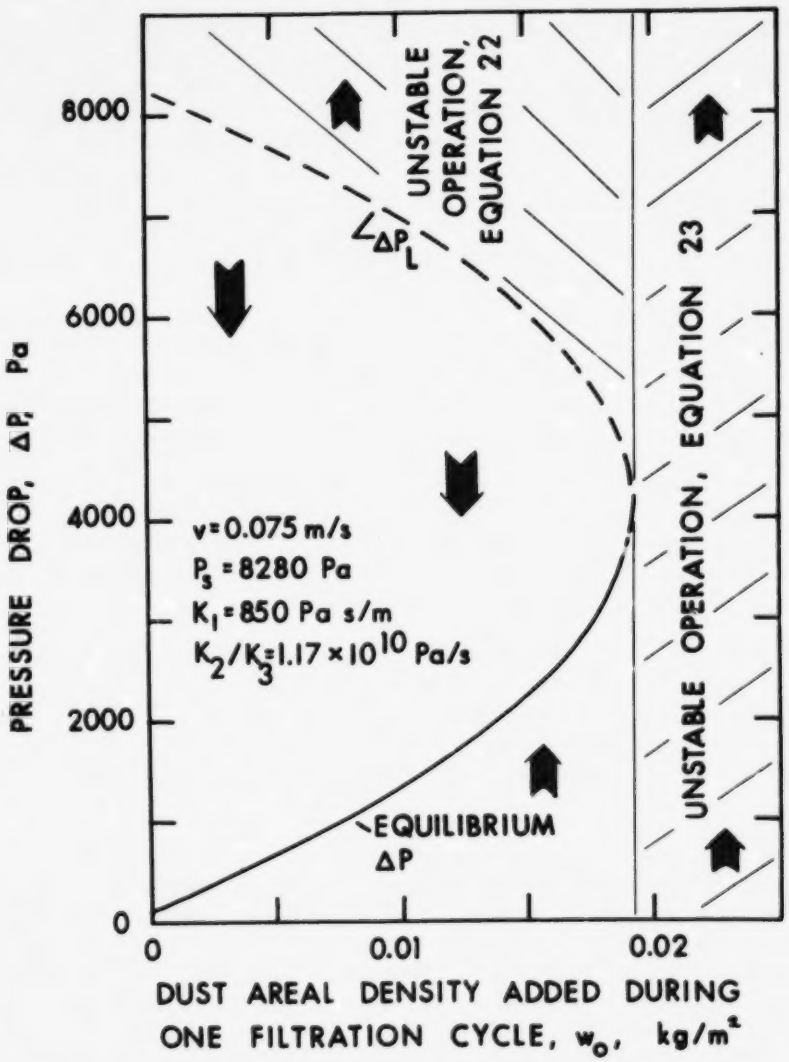

Figure 6-2. Pressure drop, ΔP, vs. dust areal density added during one filtration cycle, w_0.

6.4 mm (¼") jet discharging into a standard pulse-jet venturi using the apparatus shown in Figure 6-3. Compressed air was injected continuously and the no-flow static pressure across the venturi, P_s, measured. Results of these tests for several pulse pressures are given in Figure 6-4, and are described by:

$$P_s(\text{Pa}) = 164\ P(\text{kPa})^{0.6} \qquad (6\text{-}27)$$

Pulse pressure, P, in pounds per square inch is converted to kPa through multiplication by 6.9.

Equation (6-20) for equilibrium pressure drop requires values for operating variables w_0, v, and P_s as well as for constants K_1, K_2/K_3, and K_4/K_3. Data on the pressure drop characteristics of a three bag pulse-jet filter operated at four filtration velocities from 50 to 125 mm/s have been reported and discussed in detail elsewhere(14), and are summarized in Table 6-1. The test dust was fly ash collected electrostatically at a coal-fired utility boiler.

Examination of Equations (6-7) and (6-8) shows that:

$$K_4/K_3 = v^* w_b/t_i \qquad (6\text{-}28)$$

Dennis and Wilder(12) determined that the maximum outward velocity, v^*, attained by one polyester felt bag laden with fly ash is 1.4 m/s, and that the time necessary to reach this velocity was about 5.5 milliseconds. If the clean fabric has an areal density of 0.54 kg/m^2, the value of K_4/K_3 from Equation (6-28) is 137 Pa, less than 2% of P_s from which it is subtracted in Equation (6-20) to calculate equilibrium pressure drop. In this case, K_4/K_3 may perhaps be neglected, making subsequent analysis much simpler. The size of the error introduced by this assumption is not well established, but may be small unless the filter is operated in an unstable or nearly unstable manner.

If K_4/K_3 is neglected, then Equation (6-20) for equilibrium pressure drop involves as constants only K_1 and the ratio K_2/K_3. Lacking other data, the resistance of the conditioned fabric, K_1, might be approximated from the inverse of clean fabric Frasier permeability, F:

$$K_1(\text{Pa}\cdot\text{s/m}) = \frac{24{,}500}{F\ (\text{cfm/ft}^2 \text{ at } \tfrac{1}{2} \text{ inch of water})} \qquad (6\text{-}29)$$

The consequence of this assumption is to incorporate all pressure drop beyond that across the clean fabric into the term for resistance across the dust deposit. Although this approximation may not be realistic for conditioned fabrics which retain an appreciable amount of dust, it does allow the analysis to proceed when data on the actual resistance of the conditioned fabric are unavailable.

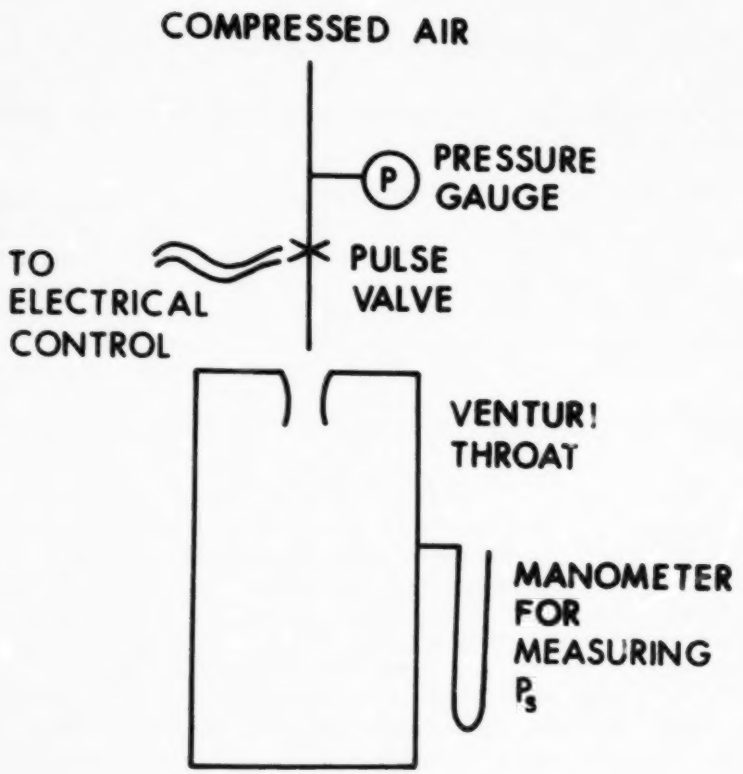

Figure 6-3. Apparatus used to determine relationship between pulse pressure, P, and induced static pressure, P_s.

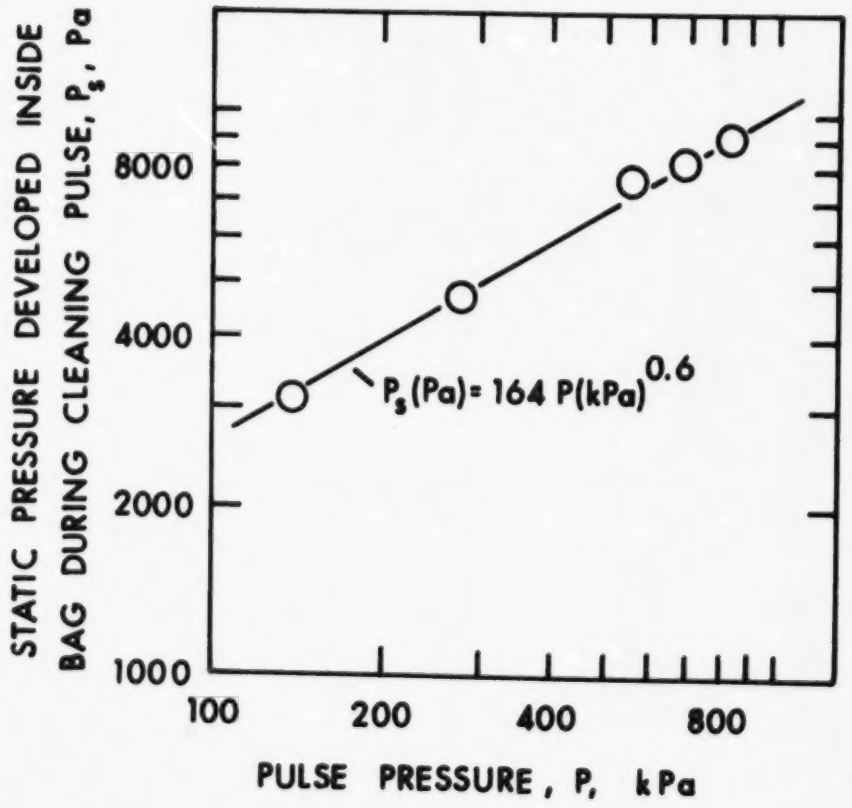

Figure 6-4. Static pressure induced, P_s, vs. pulse pressure.

Table 6-1. EXPERIMENTAL CONDITIONS FOR PULSE-JET FILTER TESTS

Bags	
Number:	3
Size:	114 mm dia. and 2.44 m long
Fabric:	polyester felt, no surface treatment
Weight:	0.54 kg/m^2 (16 oz/yd^2)
Permeability:	30 cfm/ft^2 at ½ inch of water
K_1:	850 Pa·s/m (new fabric)
Pulses	
Frequency	once per minute to each bag
Pulse Pressure, P:	690 kPa (100 psig)
Induced Pressure, P_s:	8280 Pa (33 inches H_2O)
Dust	
Type:	Fly ash precipitated from coal-fired utility boiler
Count Median Diameter:	0.30 μm
Geometric Standard Deviation:	2.7
w_0:	3.1 x 10^{-3} kg/m^2

Pressure Drop

Velocity, mm/s	ΔP, Pa	K_2/K_3, Pa/s	K_4/K_3, Pa
50	260	1.13 x 10^{10}	assumed equal
75	390	1.11 x 10^{10}	to zero, all
100	615	1.31 x 10^{10}	conditions
125	790	1.32 x 10^{10}	
Average:		1.17 x 10^{10}	0

If K_1 is known or assumed, and if equilibrium pressure drop is known for one set of stable operating conditions, then K_2/K_3 can be determined and pressure drop under any other stable operating conditions can be found using Equation (6-20). Values of K_2/K_3 were determined in this way for pressure drop at each velocity listed in Table 6-1. The values of K_2/K_3 were found to be relatively constant over the range of filtration velocities considered.

Figure 6-5 is a plot of pressure drop against filtration velocity for the data in Table 6-1. The line is based on Equation (6-20), with K_2/K_3 equal to its average value for these data, and reflects well the trend of pressure drop vs. velocity given by the

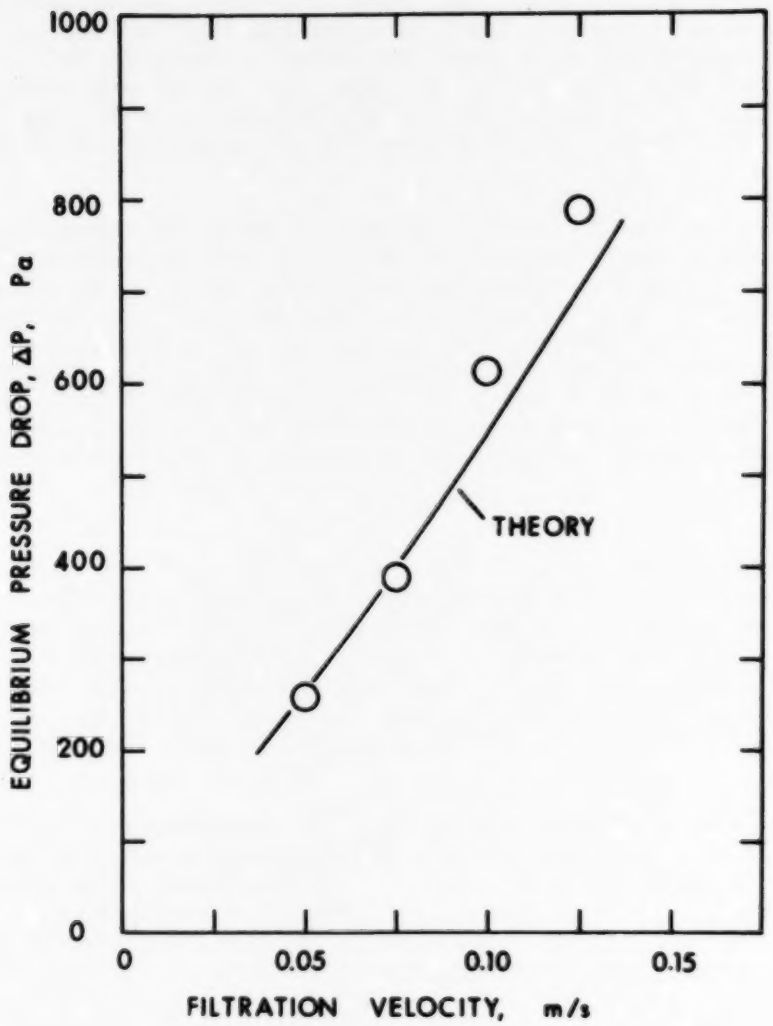

Figure 6-5. Equilibrium pressure drop, ΔP, vs. filtration velocity, v.

data. This analysis gives no indication whether agreement between theory and data will be as good for variations in variables other than filtration velocity.

The constants listed in Table 6-1 are specific for the apparatus and experimental conditions used in their determination. Changes in pulse pressure or changes in amount of dust fed to the bags between pulses were not made in these experiments. However, Equation (6-20) can be used to estimate the effect on pressure drop of variations in these variables. Results are plotted in Figures 6-6 and 6-7, pressure drop vs. pulse pressure and w_0, respectively. In Figure 6-6, pulse pressure converted to P_s using Equation (6-27) before the theoretical pressure drop line was plotted.

Equation (6-1) relates pressure drop to these variables empirically and was established for fly ash collected on polyester felt bags. However, the dust and bags used to develop the constants used in the theoretical analysis were different. The slopes of the pressure drop vs. pulse pressure and pressure drop vs. w_0 relationships predicted by the empirical equation are also given in Figures 6-6 and 6-7. The lines given by the theory and the empirical results are in general agreement. A more complex test of the theory presented here awaits development of more data.

SUMMARY

A theory for pressure drop in pulse-jet cleaned filters has been presented. Assumptions made are that total pressure drop is the sum of drops across the conditioned fabric and the dust deposit, that the fraction of dust separated from a bag depends upon the separation force applied, and that this force can be found from impulse and momentum considerations as the bag and dust deposit move away from their supporting cage during a cleaning pulse.

The theory allows prediction of operating conditions under which filter operation will become unstable and cause pressure drop to increase without limit. With simplifying assumptions, the theory can be used to interpret pressure drop data or to predict the equilibrium pressure drop of a pulse-jet cleaned filter operated under any operating conditions.

NOMENCLATURE

A	fabric area, m^2
a	see equation (6-12)
b	see equation (6-13)
c	see equation (6-14)
c_i	dust inlet concentration, kg/m^3
F	Frasian permeability (cfm/ft^2 @ 1/2" H_2O)
$F(N)$	see equation (6-17)
F_s	force acting to separate dust deposit from fabric, N

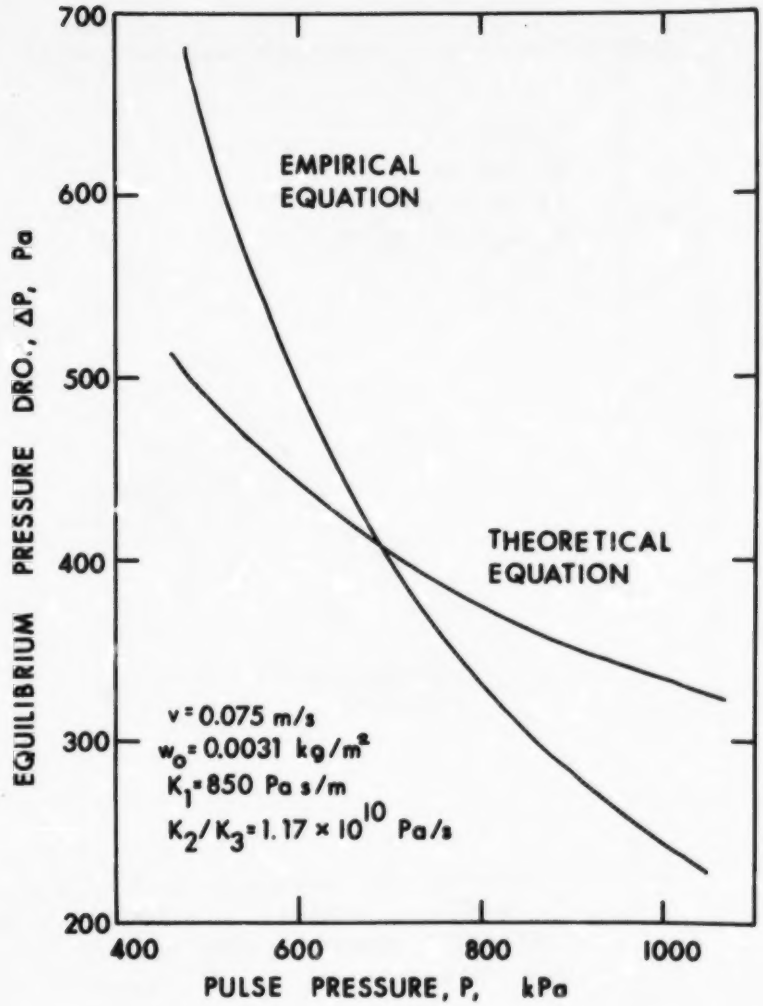

Figure 6-6. Equilibrium pressure drop, ΔP, vs. pulse pressure, P.

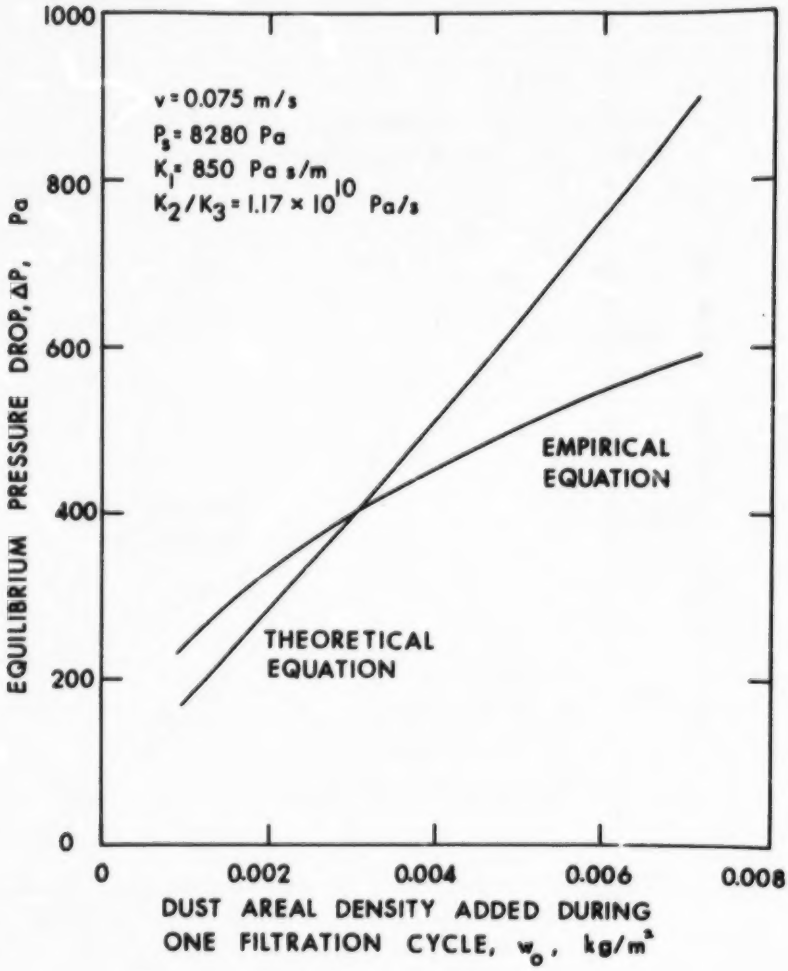

Figure 6-7. Equilibrium pressure drop, ΔP, vs. areal dust density added during one filtration cycle, w_0.

K_1	fabric resistance, Pa·s/m
K_2	specific resistance of dust deposit, s^{-1}
K_3	constant, see equation (6-8)
K_4	constant, see equation (6-8)
k	proportionality constant, see equation (6-3)
N	number of filtration cycles
P	pulse pressure, kPa
P_s	maximum static pressure developed inside bag as result of cleaning pulse, Pa
q	see equation (6-15)
t	time between pulses to each bag, s
t_1	time during which ΔPr acts, s
t_2	time during which Fs acts, s
v	superficial filtration velocity, m/s
v*	maximum velocity achieved by fabric and dust during cleaning, m/s
w	areal density of dust deposit, kg/m^2
w_b	areal density of fabric, kg/m^2
w_i	dust deposit areal density at N=0, when operating conditions change
w_0	dust areal density added during one filtration cycle, kg/m^2
Δp	pressure drop across bag and dust deposit, Pa
Δp_i	pressure drop at N=0, when operating conditions change, Pa
Δp_L	minimum Δp_i if stable operation is to be attained, Pa
Δp_r	difference between static pressure inside and outside the bag during cleaning, $P_s-\Delta p$, Pa
ε	fraction of the dust deposit removed from a fabric

REFERENCES

1. Carman, P. C. Fluid Flow Through Granular Beds. Trans. Inst. Chem. Eng., 15:150, 1937.

2. Williams, C., T. Hatch and L. Greenburg. Determination of Cloth Area for Industrial Filters. Heat. Piping Air Cond., 12(4):259, 1940.

3. Stephan, D. G., G. W. Walsh and R. A. Herrick. Concepts in Fabric Air Filtration. Am. Ind. Hyg. Assoc. J., 21(1):1, 1960.

4. Pich, J. Pressure Characteristics of Fibrous Aerosol Filters. J. Colloid Interface Sci., 37(4):912, 1971.

5. Rudnick, S. N. Fundamental Factors Governing Specific Resistance of Filter Dust Cakes. Sc.D. Thesis, Harvard School of Public Health, Boston, Ma., 1978.

6. Rudnick, S. N. and M. W. First. Specific Resistance (K_2) of Filter Dust Cakes: Comparison of Theory and Experiments. 3rd Symposium on Fabric Filters for Particle Collection. EPA-600/7-78-087, NTIS, Springfield, Va., 1978.

7. Happel, J. Viscous Flow in Multiparticle Systems: Slow Motion of Fluids Relative to Beds of Spherical Particles. AIChE J., 4(2):196, 1958.

8. Billings, C.E. and J. Wilder. Handbook of Fabric Filter Technology. Volume I. Fabric Filter Systems Study. NTIS Number PB-200-648, Springfield, Va., 1970.

9. Davis, W. T., P. J. LaRosa and K. E. Noll. The Generation and Evaluation of Fabric Filter Performance Curves from Pilot Plant Data. Filtr. Sep., 13(6):555, 1976.

10. Robinson, J. W., R. E. Harrington and P. W. Spaite. A New Method for Analysis of Multicompartmented Fabric Filtration. Atmos. Environ., 1(4):499, 1967.

11. Dennis, R., R. W. Cass and R. R. Hall. Dust Dislodgement from Woven Fabrics Versus Filter Performance. J. Air Poll. Control Assoc., 28(1):47, 1978.

12. Dennis, R. and J. Wilder. Fabric Filter Cleaning Studies. EPA-650/2-75-009, NTIS, Springfield, Va., 1975.

13. Dennis, R., R. W. Cass, D. W. Cooper, R. R. Hall, V. Hampl, H. A. Klemm, J. E. Langley and R. W. Stern. Filtration Model for Coal Fly Ash with Glass Fabrics. EPA-600/7-77-084, NTIS, Springfield, Va., 1977.

14. Ellenbecker, M. J. Pressure Drop in a Pulse-Jet Fabric Filter. Sc.D. Thesis, Harvard School of Public Health, Boston, Ma., 1979.

15. Ellenbecker, M. J. and D. Leith. Pressure Drop in a High Velocity Pulse-Jet Fabric Filter. Paper 78-62.6 presented at the 71st Annual Meeting of the Air Pollution Control Association, Houston, Tx., 1978.

16. Leith, D., M. W. First and H. Feldman. Performance of a Pulse-Jet Filter at High Filtration Velocity II. Filter Cake Redeposition. J. Air Poll. Control Assoc., 27(7):636, 1977.

17. Leith, D., D. D. Gibson, and M. W. First. Performance of Top and Bottom Inlet Pulse-Jet Fabric Filters. J. Air Poll. Control Assoc., 28(7):696, 1978.

18. Dennis, R. and L. Silverman. Fabric Filter Cleaning by Intermittent Reverse Air Pulse. ASHRAE J., 4(3):43, 1962.

19. Leith, D. and M. W. First. Pressure Drop in a Pulse-Jet Fabric Filter. Filtr. Sep., 14(5):473, 1977.

20. Strangert, S. Predicting Performance of Bag Filters. Filtr. Sep., 15(1):42, 1978.

SECTION 7

HIGH VELOCITY FIBROUS FILTRATION

INTRODUCTION

Mats of fibrous materials have been used for many years to collect particles from gas streams(1). Several different collection mechanisms, including diffusion, impaction, and interception, can contribute to the overall collection efficiency of fibrous mats. These collection mechanisms are well understood, and the theories describing them can be used to accurately predict collection efficiency over a wide range of filter and operating characteristics.

The theory and experiments described here are concerned with a set of filtration conditions which are outside the range of "normal" filtration. The predominant characteristic of this filtration regime is the very high filtration velocities used - in the range of 1-10 m/s (200-2,000 fpm). These filtration velocities, when combined with the tested filter materials (randomly oriented 8 μm stainless steel fibers) and dust (resuspended fly ash), result in particle collection characteristics which cannot be described satisfactorily by classical filtration theory.

This combination of particle sizes, fiber diameter, and filtration velocities results in particle collection predominantly by impaction, even for very small particles. Just as importantly, the kinetic energy of large particles and the drag forces on collected agglomerates are sufficiently large so that particle bounce and reentrainment can be expected.

This research was undertaken to investigate fly ash collection characteristics in the high inertia regime. In particular, the research is aimed at determining combinations of fiber beds and filtration conditions where small particles are effectively collected by impaction while large particles bounce through or are reentrained. Since the large particles which would penetrate such a filter can be collected by other simple devices (e.g., cyclones), this penetration characteristic could possibly form the basis for a two-stage, high efficiency collection device.

THEORY

Particle Collection Mechanisms

Introduction--

Filtration theory attempts to predict overall particle removal in a filter based on an understanding of the interaction of particles with a single filter element. This element can be an isolated fiber or previously collected dust particles.

The single element efficiency, η_s, is defined as the number of particles collected by a filter element divided by the number of particles whose centers pass through the element's projected area as the particles approach it(2). The major mechanisms by which particles collect in a filter element are inertial impaction, diffusion, interception, gravity settling, and electrostatic deposition(2).

Inertial Impaction--

As the gas flows past a collector element, the streamlines curve around the collector. Near the collector surface, inertia will cause particles to deviate from the streamlines. Particles with sufficient inertia can cross streamlines and hit the collector. Inertial impaction has been found to be proportional to the dimensionless impaction parameter(2), ψ:

$$\psi = \frac{\rho_p d_p^2 v C_c}{18 \mu d_f} \qquad (7\text{-}1)$$

where:
- ρ_p = particle density (kg/m^3)
- d_p = particle diameter (m)
- v = superficial filtration velocity (m/s)
- C_c = Cunningham slip correction factor
- μ = gas viscosity (Pa·s)
- d_f = fiber diameter (m)

Much experimental and theoretical work has been devoted to determining the relationship between the impaction parameter, ψ, and the single fiber collection efficiency from impaction, η_I. One widely accepted empirical formula was derived from experiment and theory by Landahl and Herrmann(3). It was developed for a fiber Reynold's Number of 10 and can be expressed as(2):

$$\eta_I = \frac{\psi^3}{\psi^3 + 0.77\psi^2 + 0.22} \qquad (7\text{-}2)$$

Typical Calculations--

Theoretical impaction collection efficiencies can be calculated for values of the variables used in this study, which are

summarized in Table 7-1. All experiments were conducted using 8 μm diameter fibers. Figure 7-1 plots single fiber collection efficiency η_I as a function of particle size for the lowest velocity (1 m/s) and the highest velocity (10 m/s) used here. Note that a significant fraction of even very small particles will impact a fiber at these velocities.

Other Collection Mechanisms--

Since the fibers used in this study were very small (8 μm diameter), interception might be thought to be important. However, velocities were sufficiently high so that impaction always completely overshadowed interception. The theoretical single fiber collection efficiency from impaction and interception combined was calculated assuming that the mechanisms are independent but that a particle caught by one mechanism cannot be caught by the other(4); the combined collection efficiency never exceeded the single fiber collection efficiency from impaction alone by more than 1%. Likewise, particle collection from diffusion was negligible under the conditions considered.

Overall Collection Efficiency

Dorman(5) gives the overall collection efficiency for a filter of thickness L and solidity α as:

$$\eta = 1 - \mathrm{Exp}\left[\frac{-4L\alpha\eta_s}{\pi d_f(1-\alpha)}\right] \qquad (7\text{-}3)$$

where η_s is the combined single fiber collection efficiency from all effects. In this study, impaction dominates all other collection mechanisms so that

$$\eta_s \simeq \eta_I \qquad (7\text{-}4)$$

Equation(7-3)is difficult to apply in this case, because at the high velocities used here the filter mats compress and L changes in a manner which is difficult to measure and/or predict. However, Equation (7-3) can be modified by making use of the definition of solidity, α, defined as the ratio of fiber volume to total filter volume:

$$\alpha = \frac{V_f}{V_T} = \frac{m_f/\rho_f}{LA} \qquad (7\text{-}5)$$

$$\alpha = \frac{m_f}{\rho_f LA} \qquad (7\text{-}6)$$

where ρ_f is the filter density and m_f and A are the filter mass and cross-sectional area, respectively. Solving Equation (7-6)

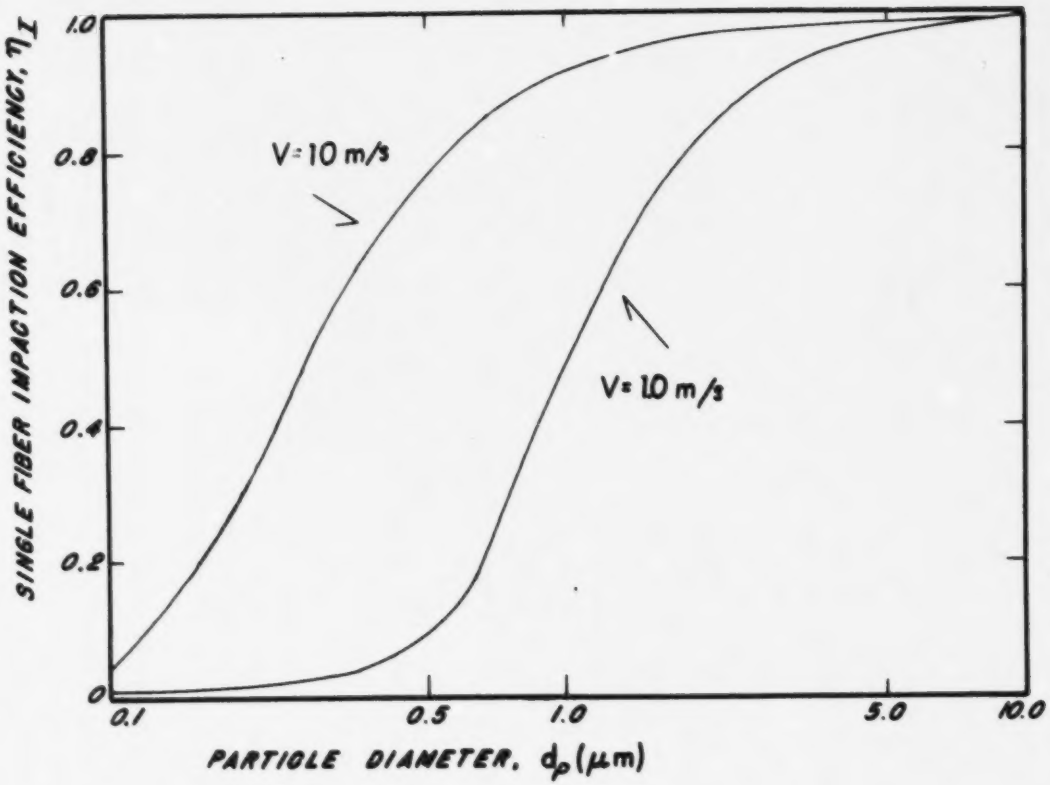

Figure 7-1. Theoretical single fiber impaction efficiency vs. particle diameter at 1 and 10 m/s filtration velocities.

for filter thickness L and substituting into Equation (7-3):

$$\eta = 1 - \text{Exp}\left[\frac{-4m_f\eta_I}{\pi\rho_f d_f A(1-\alpha)}\right] \qquad (7\text{-}7)$$

The overall theoretical filter collection efficiency can thus be calculated from easily measured filter bed parameters (m_f, ρ_f, d_f, A), the theoretical single fiber collection efficiency from impaction (η_I), and filter porosity ($1-\alpha$). Porosity changes with filtration velocity; however, the porosity of a filter with no airflow can be measured using pycnometry, and changes in porosity with filtration velocity can be estimated from the slope of the measured pressure drop versus velocity curve.

EXPERIMENTAL APPARATUS

Apparatus

Figure 7-2 is a diagram of the experimental high velocity filtration system. It contains a 30 cm square filter holder by which fibrous materials can be packed to depths of up to 15 cm. A movable 4-mesh screen upstream and a stationary 4-mesh screen downstream provide rigid support at high filtration velocities. A downstream centrifugal blower draws the test aerosol through the 20 cm round entry duct, the filter holder, and the Venturi meter which measures the airflow rate. A Dwyer photohelic gauge is used with a motor driven blastgate to maintain a constant airflow rate.

A National Bureau of Standards (NBS) dust feeder(6) generates the fly ash aerosol at mass rates from 3 to 125 g/min. The test dust is an electrostatically precipitated fly ash with a count median diameter (CMD) of 0.14 μm and a geometric standard deviation (GSD) of 1.9. A polydisperse (CMD = 0.7 μm, GSD = 2.05) dioctyl phthalate (DOP) aerosol can also be generated using a DeVilbiss nebulizer (The DeVilbiss Co., Somerset, PA). The test aerosol and inlet air are thoroughly mixed before entering the filled section by a Stairmand disk(7) located at the inlet duct.

Simultaneous up and downstream isokinetic samples are taken to determine aerosol penetration of the filter medium. Microscopic and gravimetric analyses of the sample filters determine particle size distribution of the fly ash and downstream of the filtering section as well as overall collection efficiency. Eight stage Anderson impactors (Anderson-2000 Inc., Atlanta, Georgia) are also up and downstream for particle sizing. DOP penetration is measured using a Particle Measuring Systems, Inc., laser scattering aerosol spectrometer (PMS Model CSASP-100).

Procedures

Upon packing a filter material into the filter housing and

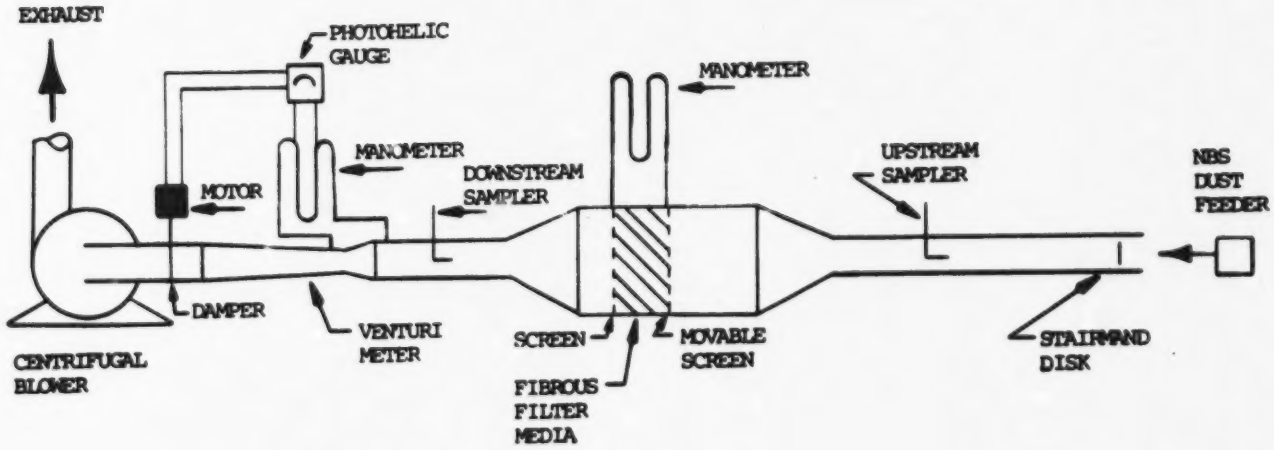

Figure 7-2. High velocity filtration apparatus.

setting the airflow rate, test aerosol is generated and directed to the filter. Inlet dust concentration is held constant and after the filter reaches maximum pressure drop (about 7.5 kPa) the filter is removed for inspection and cleaning. During the dust loading, pressure drop across the filter is recorded and aerosol samples are taken at regular intervals. Cleaning of the filter material can be done by blowing compressed air through the upstream side of the filter, striking the filter and filter frame against a rigid surface, or shaking the filter manually. After cleaning, the filter is placed in the filter housing and retested at original flow rate and dust loading.

EXPERIMENTS

The fractional penetration of fly ash through filter mats of 8 μm stainless steel fibers was measured at five filtration velocities: 1.5, 2.9, 3.2, 6.9 and 8.0 m/s. The characteristics of the fly ash and filter material are given in Table 7-1. At the lower velocities the filtration time between cleanings was long enough so that adequate Anderson impactor samples could be collected in one cleaning cycle, while at the higher velocities multiple cycles were needed to obtain sufficient impactor deposits.

TABLE 7-1. VALUES OF TEST VARIABLES USED IN THIS STUDY

Dust	
Type	resuspended fly ash
Count median diameter	0.14 μm
Geometric standard deviation	1.9
Particle density (ρ_p)	2.2×10^3 kg/m^3
Filter	
Fiber type	310 stainless steel
Fiber diameter (d_f)	8 μm
Fiber density (ρ_f)	7.92×10^3 kg/m^3
Filter cross-sectional area(A)	0.093 m^2
Filter mass, m_f	0.032 kg
Filtration velocity (V)	1 - 10 m/s

The fractional penetration of the polydisperse DOP aerosol was also measured over the same velocity range. The DOP concentration was extremely low, so that the filter exhibited no loading effects during the DOP tests.

RESULTS

Fractional penetration curves for fly ash collected at five different filtration velocities are presented in Figure 7-3. Increased penetration with both velocity and particle size is evident.

Similar measurements were made with the liquid DOP aerosol at six velocities; the fractional penetration curves for these experiments are shown in Figure 7-4. Shown also for comparison in Figure 7-4 are the 1.5 and 8.0 m/s fly ash penetration curves from Figure 7-3. In contrast to the fly ash, the DOP aerosol penetration follows the trends predicted by classical impaction theory, decreasing with both velocity and particle size.

Dust concentration downstream of filters loaded with fly ash using clean inlet air were also measured and found to be insignificant at these velocities.

DISCUSSION

Particle Bounce

Equation (7-7) is a theoretical formula which predicts overall filter collection efficiency (η) from the single fiber collection efficiency (η_I) and gross filter parameters (m_f, ρ_f, d_f, A, $1-\alpha$). However, Equation (7-7) can also be used to calculate experimental single fiber collection efficiencies (η'_I) from experimental filter collection efficiency data (η'). Such numbers are more useful than overall collection efficiencies in comparing results to theory because they are independent of the particular filter configuration tested and should only be a function of the particle-fiber impaction parameter (Equation 7-2).

Solving Equation (7-7) for η'_I,

$$\eta'_I = - \frac{\pi \rho_f d_f A(1-\alpha)\ln(1-\eta')}{4m_f} \qquad (7\text{-}8)$$

and substituting the filter parameters from Table 7-1 gives:

$$\eta'_I = -0.145(1-\alpha)\ln(1-\eta') \qquad (7\text{-}9)$$

where the solidity, α, is a function of filtration velocity. As discussed earlier, changes in α with velocity can be estimated from the clean filter pressure drop curve; in any case, the quantity $1-\alpha$ is always close to unity in these tests so that changes in α have little effect on the calculation of η'_I.

The empirical formula of Landahl and Herrmann relating impaction parameter (ψ) and η_I (Equation 7-2) is plotted in Figure 7-5.

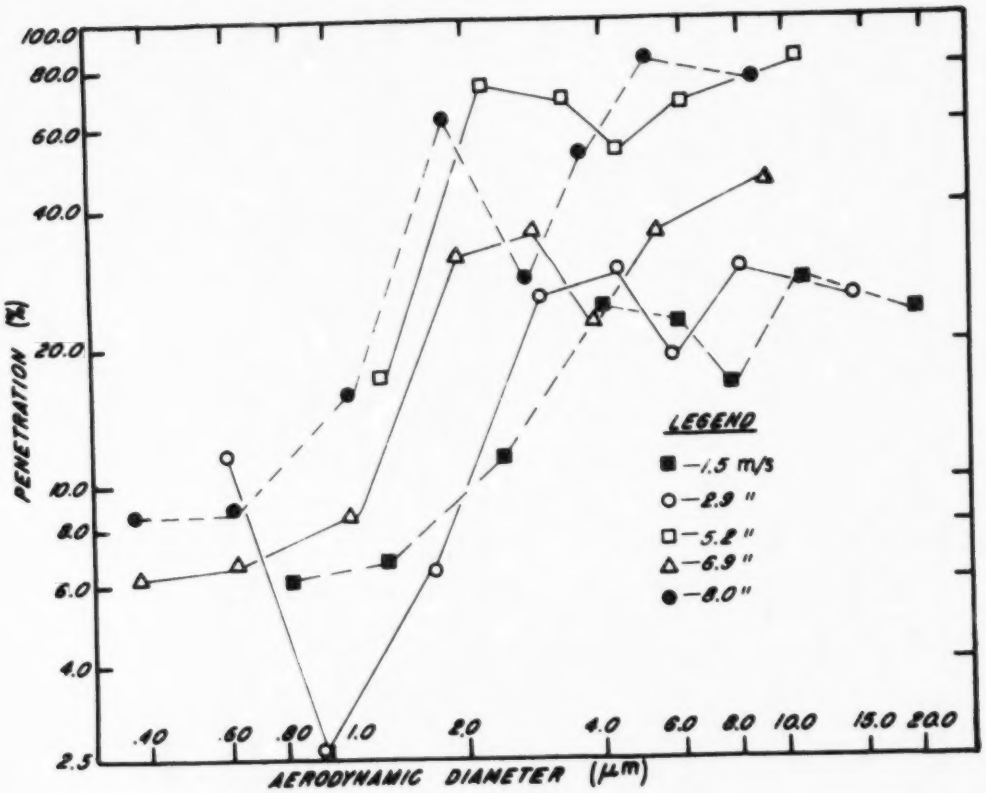

Figure 7-3. Fly ash penetration vs. particle size at five filtration velocities.

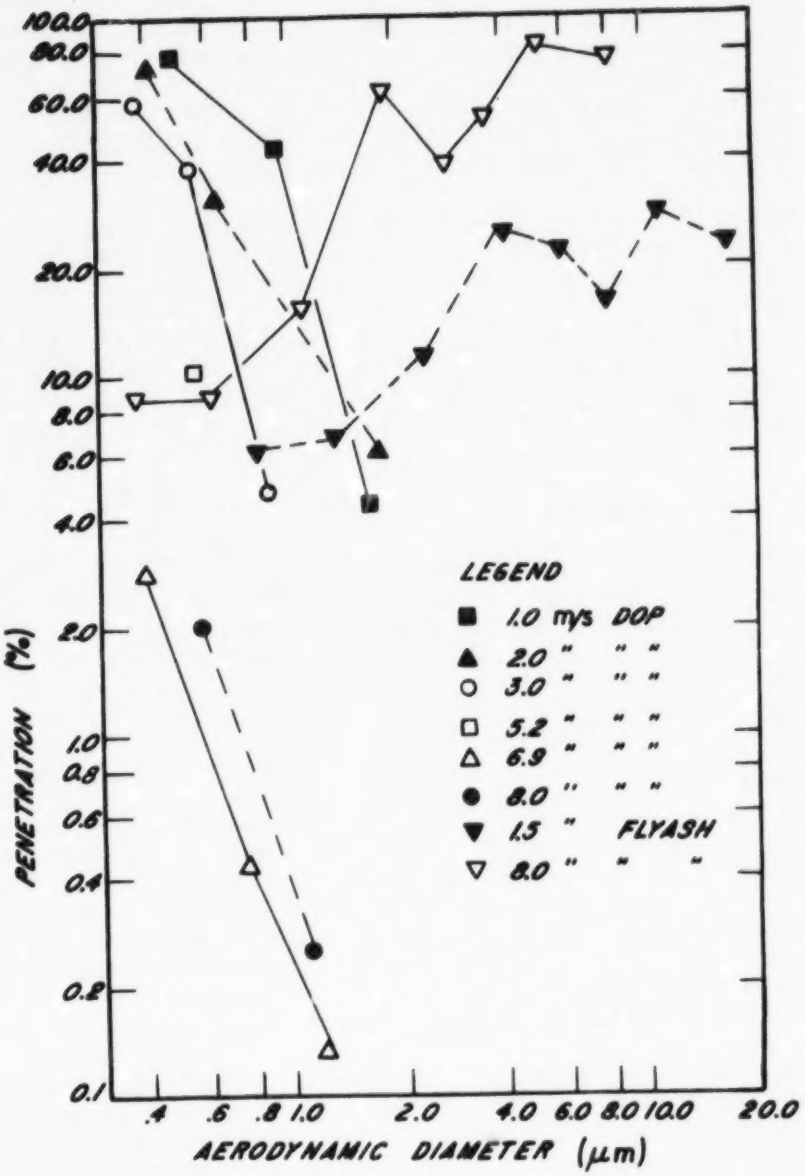

Figure 7-4. Dioctyl phthalate (DOP) penetration vs. particle size at six filtration velocities.

Also plotted are the experimentally determined single fiber collection efficiencies for the lower test velocity (1.5 m/s, $\alpha = 0.0085$) and the highest test velocity (8.0 m/s, $\alpha = 0.0285$). The values for intermediate velocities are similar and have been omitted for simplicity. As shown in Figure 7-5, the experimental and theoretical single fiber collection efficiencies are in agreement only for the smallest Anderson impactor fly ash size category, when the fiber impaction parameter is approximately equal to 1. As impaction parameter increases the experimental η'_I decreases; when η_I equals 0.99 ($\psi \simeq 100$), η'_I equals only 0.2 for the lowest velocity and 0.05 for the highest velocity.

Experimental single fiber collection efficiency data for the liquid DOP aerosol are also shown in Figure 7-5. In contrast to the fly ash data, the DOP η'_I values closely fit the Landahl and Herrmann curve. These data strongly suggest that fly ash particles do impact the fibers but bounce through the filter at high velocities. Indeed, for particles larger than 4 μm the data indicate that approximately 80% of the particle-fiber collisions result in particle bounce at 1.5 m/s and that 95% result in particle bounce at 8 m/s.

Adhesion Probability

The amount of particle bounce for different velocities and particle sizes is indicated by the particle adhesion parameter, h, which is defined as the probability of a particle adhering to a fiber after colliding with it(8). Theoretically, the probability of particle adhesion can be calculated from a consideration of the energies involved. A particle will not adhere to a fiber upon collision if the kinetic energy of the particle on rebound is greater than the energy of attraction (primarily due to London van der Waals forces)(9). Löffler(8) and Dahneke(9) present the energy balance equation and the procedures for calculating critical conditions necessary for bounce to begin. As pointed out by Dahneke(9) and Esmen, et al.(10), the equations are difficult to solve for a polydisperse, irregular dust such as fly ash and a multilayer fiber filter, so that adhesion probability cannot be predicted as a function of particle size and velocity. However, experimentally measured adhesion probability should show a correlation with particle kinetic energy.

The adhesion probability can be obtained from experimental data by taking the ratio of the experimentally measured single fiber collection efficiency to the theoretical single fiber collection efficiency. Since impaction predominates in this study,

$$h = \frac{\eta'_I}{\eta_I} \qquad (7\text{-}10)$$

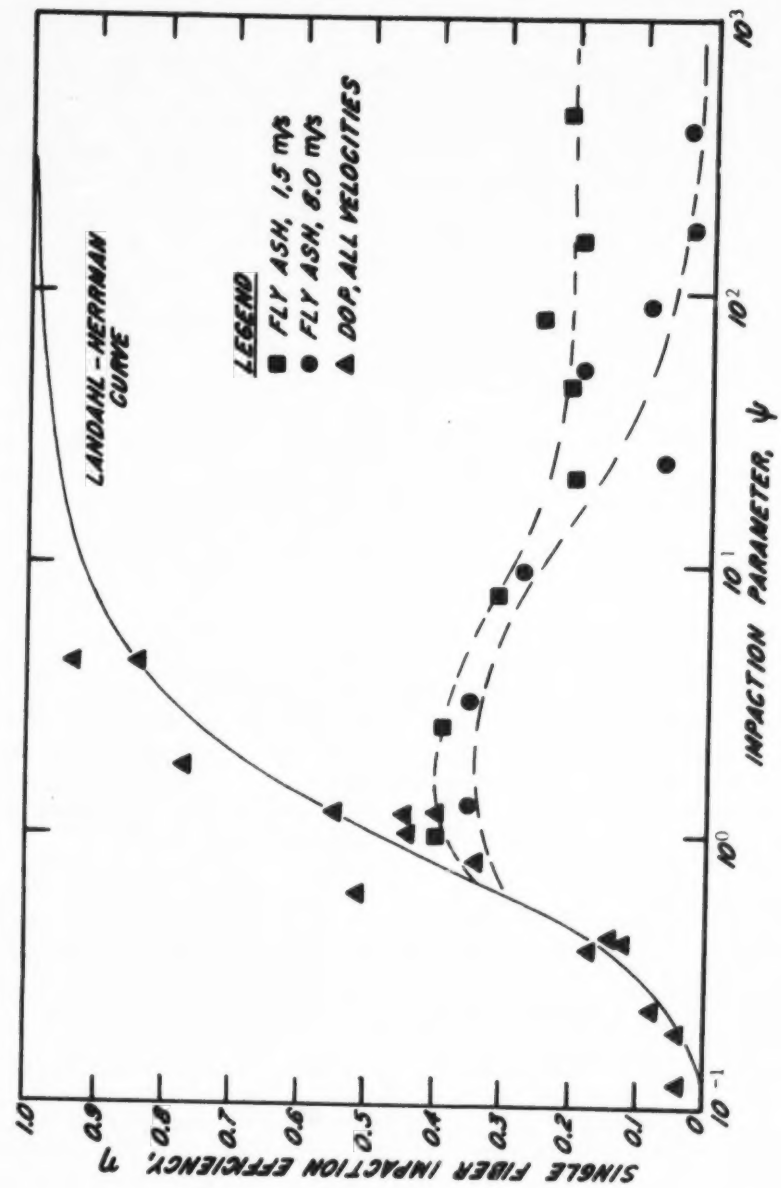

Figure 7-5. Theoretical and experimental single fiber impaction efficiencies vs. impaction parameter for DOP and fly ash.

The adhesion probabilities calculated for all of the data points in Figure 7-3 are plotted against particle kinetic energy in Figure 7-6. The expected decrease in adhesion probability with increasing kinetic energy is evident. The data fall on a straight line (log-log plot) at low energies (high adhesion probability) but exhibit increasing scatter at higher energies (low adhesion probability).

The spread in data at high energies may be caused by the complex particle impaction and rebound pattern which would exist in this regime. High energy particles, after bouncing, will accelerate until reaching gas velocity; during acceleration they may impact another fiber and rebound again or they may adhere, depending on the velocity at impact. A very complex collection pattern can thus be expected for a polydisperse dust in a multilayer filter for particles with large kinetic energy. However, this mechanism cannot account for the very low adhesion probabilities measured on two experiments (v = 5.2 m/s and 8.0 m/s) when the particle kinetic energy exceeded 10^{-13} J. Additional data will be collected in an attempt to clarify these results.

Relative humidity can have a great effect on particle adhesion(11), and thus could have contributed to the differences in adhesion probabilities measured in different experiments. Relative humidity ranged from 20-50% during the experiments, but the adhesion data could not be correlated with the relative humidity data.

A regression line was fit to the data of Figure 7-6 and is plotted in Figure 7-7. Also plotted are data of Löffler(8) and Esmen, et al.(10). Löffler's data were collected for 1.8-10.0 μm diameter NaCl particles collected on 20 μm diameter polyamide fiber filters while Esmen, et al., impacted 4.4 and 8.8 μm diameter uranine spheres on a flat brass substrate. Considering the different particles and substrates used, the agreement among the various experiments is good. Figure 7-7 indicates a region of particle inertial energy where particle adhesion can be expected to be very good ($E_K > 10^{-13}$J). In the intermediate energy regime, (10^{-15}J < E_K < 10^{-13}J), particle adhesion probability will be a strong function of the particular particle and filter used.

Practical Design Implications

The penetration characteristics reported here suggest that a novel, compact, high efficiency particle collector may be feasible. The device would operate at high gas velocities, and would collect particles over a wide size range by impaction. It would consist of two stages: 1) a fibrous media filter, which would efficiently collect small particles but allow some particles to bounce through or reentrain; and 2) a cyclone, which can efficiently collect large particles. When operated in series, the two devices should collect all particle sizes with high efficiency.

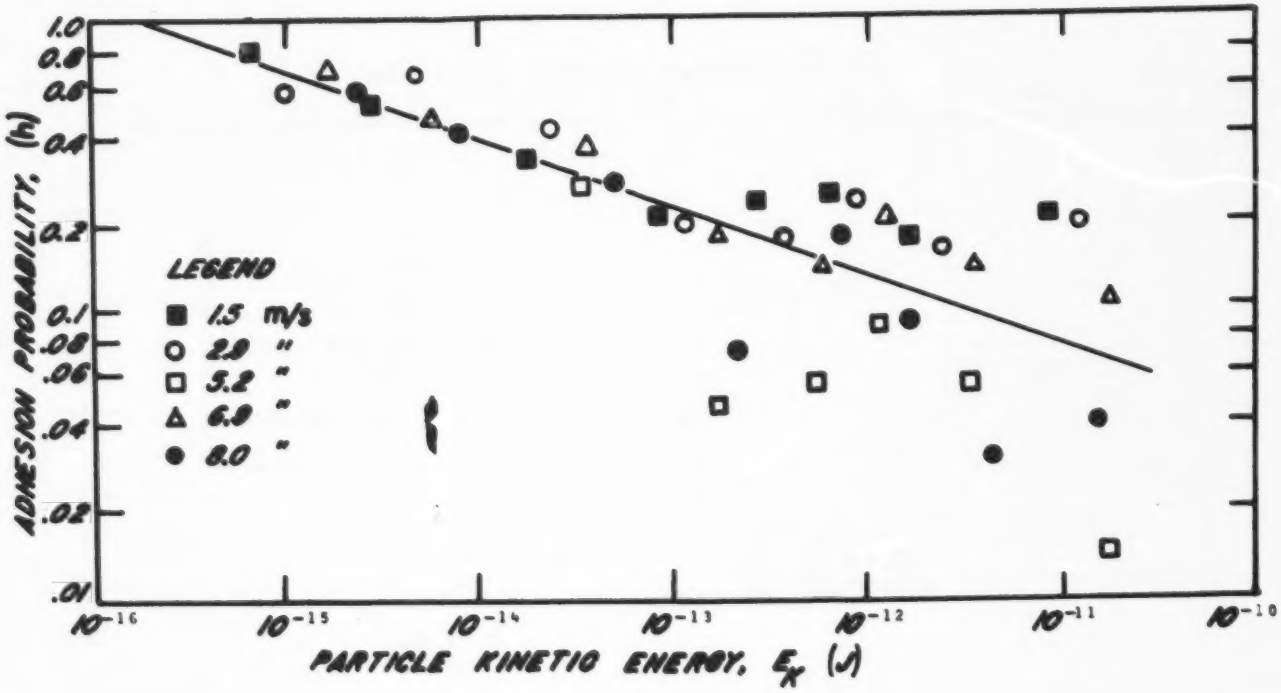

Figure 7-6. Fly ash adhesion probability vs. particle kinetic energy.

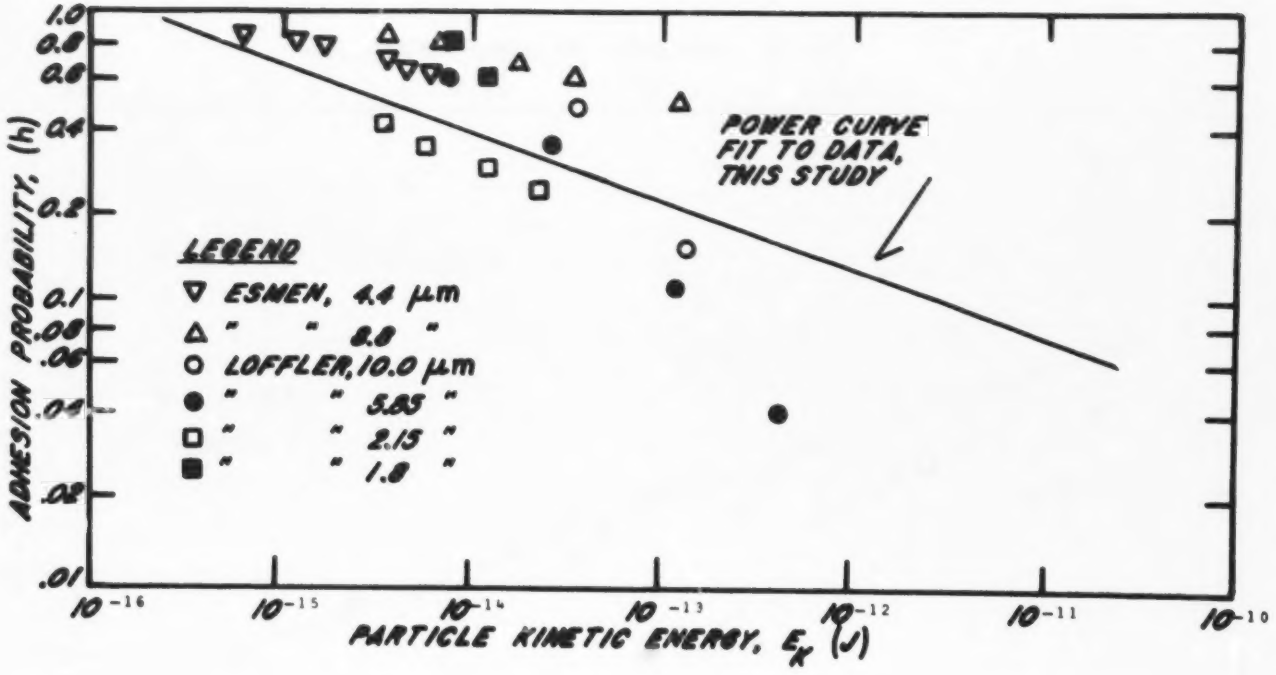

Figure 7-7. Comparison of adhesion probability data from this study with those of other investigators.

Such a device would have many desirable properties. Our experiments indicate that the pressure drop across a clean fibrous bed, when operated at high velocities, (e.g., 1.5 m/s), is about the same as across a cyclone: 0.5-1 kPa. The total pressure drop across the device would thus be fairly low - on the order of 2 kPa. The device would be extremely simple in design and easy to operate; the only area where moving parts may be needed is in the filter cleaning system, and that would depend on the cleaning method chosen. The device, by operating at high gas velocities, would be very compact. It would collect all types of aerosols (solid and liquid) and would use relatively small amounts of energy.

The design and testing of such a two-stage device is now in the planning stage. An important design consideration now being addressed is the selection of an optimum fibrous material. The ideal material would have a fractional penetration similar to the stainless steel fiber beds but would be cheaper and easier to clean in situ. Materials such as felts and sintered fiber mats are being tested in preparation for the construction of a pilot two-stage device.

SUMMARY AND CONCLUSIONS

Particle bounce has been shown to play an important role in the collection of fly ash by mats of stainless steel fibers. The penetration of fly ash particles through 8 μm fiber filters in the 1-10 m/s velocity range increased with both particle size and velocity; since impaction was the controlling collection mechanism, these results run contrary to classical filtration theory.

Particle adhesion probability was found to be inversely proportional to particle kinetic energy. This result is in general agreement with previous adhesion studies, which were performed with monodisperse aerosols under controlled laboratory conditions. This study demonstrates that the particle adhesion properties of a polydisperse dust (fly ash), under conditions similar to those encountered by practical filters, can also be related to the particle kinetic energy.

These results have important implications for the operation of fibrous filters at high velocity, and may help explain cases where penetration is higher than anticipated. These experiments also suggest the possible use of a novel two-stage inertial collection device to take advantage of the high velocity particle penetration characteristics noted here.

NOMENCLATURE

A	filter cross-sectional area, m^2
C_c	Cunningham slip correction factor
d_f	fiber diameter, m

d_p	particle diameter, m
E_K	particle kinetic energy
h	adhesion probability
L	filter thickness, m
m_f	filter mass, kg
v	superficial filtration velocity, m/s
V_f	total fiber volume, m^3
V_T	filter volume, m^3
α	filter solidity
η	theoretical filter collection efficiency
η'	experimental filter collection efficiency
η_I	theoretical single fiber impaction efficiency
η'_I	experimental single fiber impaction efficiency
η_S	combined single fiber collection efficiency
μ	gas viscosity, Pa·s
ρ_f	fiber density, kg/m^3
ρ_p	particle density, kg/m^3
ψ	inertial impaction parameter

REFERENCES

1. Davies, C. N. Air Filtration. Academic Press, Inc., New York, 1973.

2. Pich, J. Theory of Aerosol Filtration by Fibrous and Membrane Filters. In: Aerosol Science, C. N. Davies, ed. Academic Press, Inc., New York, 1966.

3. Landahl, H. D. and R. G. Herrmann. Sampling of Liquid Aerosols by Wires, Cylinders, and Slides, and the Efficiency of Impaction of the Droplets. J. Colloid Sci., 4(2):103-136, 1949.

4. Strauss, W. Industrial Gas Cleaning. 2nd ed. Pergamon Press, Oxford, 1975. p.287.

5. Dorman, R. G. Filtration. In: Aerosol Science, C. N. Davies, ed. Academic Press, Inc., New York, 1966.

6. Dill, R. S. A Test Method for Air Filters. Trans. Amer. Society of Heating and Ventilating Engin., 44:379-386, 1938.

7. Stairmand, C. J. Sampling Gas-Borne Particles. Engineering, 41:141-143, 181-183, 1941.

8. Löffler, F. Adhesion Probability in Fibre Filters. Clean Air, 8(4), 1949.

9. Dahneke, B. The Capture of Aerosol Particles by Surfaces. J. Colloid Interface Sci., 37(2):342-352, 1971.

10. Esmen, N. A., P. Ziegler and R. Whitfield. The Adhesion of Particles Upon Impaction. J. Aerosol Sci., 9:547-556, 1978.

11. Corn, M. The Adhesion of Solid Particles to Solid Surfaces, I. A Review. J. Air Poll. Control Assoc., 11(11):523-528, 1961.

TECHNICAL REPORT DATA
(Please read Instructions on the reverse before completing)

1. REPORT NO. EPA-600/7-80-042	2.
3. RECIPIENT'S ACCESSION NO.	
4. TITLE AND SUBTITLE Performance of a High-velocity Pulse-jet Filter, II	5. REPORT DATE March 1980
	6. PERFORMING ORGANIZATION CODE
7. AUTHOR(S) David Leith, M.J. Ellenbecker, M.W. First, J.M. Price, Anthony Martin, and D.G. Gibson	8. PERFORMING ORGANIZATION REPORT NO.
9. PERFORMING ORGANIZATION NAME AND ADDRESS Harvard School of Public Health 665 Huntington Avenue Boston, Massachusetts 02115	10. PROGRAM ELEMENT NO. EHE624
	11. CONTRACT/GRANT NO. Grant R804700
12. SPONSORING AGENCY NAME AND ADDRESS EPA, Office of Research and Development Industrial Environmental Research Laboratory Research Triangle Park, NC 27711	13. TYPE OF REPORT AND PERIOD COVERED Final; 9/76-9/79
	14. SPONSORING AGENCY CODE EPA/600/13

15. SUPPLEMENTARY NOTES IERL-RTP project officer is James H. Turner, Mail Drop 61, 919/541-2925. EPA-600/7-78-131 includes related work.

16. ABSTRACT The report gives results of a study of the performance of a high-velocity pulse-jet filter. Such filtration has distinct advantages over low-velocity filtration in that the equipment required to clean a gas stream is reduced in size and initial cost as velocity increases. Although high filtration velocity causes a number of problems, many of them are dealt with in the report. Location of the gas inlet to the filter was found to affect penetration and pressure drop; both were higher for inlets near the bottom of the filter housing. Fabric type was also found to affect performance by affecting the amount and characteristics of the dust deposit accumulated. Fabric surface properties help explain the nature of this deposit. These ideas and others were used to develop a mathematical model for pressure drop in a pulse-jet cleaned filter. The model can be used to predict pressure drop under stable or variable operating conditions, and to predict operating conditions that cause unstable filter operation. An understanding of particle/fiber interactions is essential to understanding the collection characteristics of a felt fabric. Under certain conditions, particles bounce on impact with fibers. An adhesion probability was determined and found to depend on incident particle kinetic energy.

17. KEY WORDS AND DOCUMENT ANALYSIS

a. DESCRIPTORS	b. IDENTIFIERS/OPEN ENDED TERMS	c. COSATI Field/Group
Pollution Filtration Pulsation Jets Fabrics Mathematical Models Felts Adhesion	Pollution Control Stationary Sources Fabric Filters Pulse-jet Filters	13B 07D 14B 20D 11E 12A

18. DISTRIBUTION STATEMENT Release to Public	19. SECURITY CLASS *(This Report)* Unclassified	21. NO. OF PAGES
	20. SECURITY CLASS *(This page)* Unclassified	22. PRICE

EPA Form 2220-1 (9-73)